ROYAL SOCIETY OF CHEMISTRY

REVIEW

Check for updates

Nanoscale MOFs in nanomedicine applications: from drug delivery to therapeutic agents

Zeyi Sun,†[ad] Tieyan Li,†[b] Tianxiao Mei,[a] Yang Liu,[c] Kerui Wu,[a] Wenjun Le*[a] and Yihui Hu [ID] *[a]

Metal–organic frameworks (MOFs) hold great promise for widespread applications in biomedicine and nanomedicine. MOFs are one of the most fascinating nanocarriers for drug delivery, benefiting from their high porosity and facile modification. Furthermore, the tailored components of MOFs can be therapeutic agents for various treatments, including drugs as organic ligands of MOFs, active metal as central metal ions of MOFs, and their combinations as carrier-free MOF-based nanodrug. In this review, the advances in delivery systems and applications as therapeutic agents for nanoscale MOF-based materials are summarized. The challenges of MOFs in clinical translation and the future directions in the field of MOFs therapy are also discussed. We hope that more researchers will focus their attention on advancing and translating MOF-based nanodrugs into pre-clinical and clinical applications.

1. Introduction

The recent decades have witnessed rapid developments and multitudinous achievements in nanomedicine. Intensive efforts have been devoted to exploiting biomaterials for pre-clinical or clinical applications,[1,2] such as diagnosis, therapy and beyond.[3-5] To date, a variety of nanomaterials have been developed as diagnostic agents, therapeutic agents, and even theranostic agents and have made enormous progress in the field of biomedicine due to their tunable size, unique surface characterizations, and high cargo loadings. Notably, nanomaterial-based agents have some intrinsic advantages over their counterparts, such as controllable release, enhanced accumulation, and augmented blood circulation, allowing for boosting the therapeutic efficacy and alleviating adverse reactions.[6] Nowadays, the vast majority of nanomaterials can be categorized into either inorganic nanomaterials, including metal-based nanomaterials, metal oxide-based nanomaterials, and carbon-based nanomaterials, or organic nanomaterials including polymer nanoparticles, liposomes, micelles, and dendrimers.[7,8] However, these nanomaterials suffer from some inherent disadvantages, such as inorganic materials that are difficult to degrade and organic materials with undesirable

cargo loadings. To tackle these challenges of purely inorganic or organic materials in biomedical applications, hybrid nano-materials have been constructed.

Nanoscale metal–organic frameworks (NMOFs) are emerging hybrid materials assembled from metal ions and organic ligands *via* coordination bonds. Importantly, they combined the benefits of inorganic and organic materials, making them more applicable in biomedicine. NMOFs possess several advantages in the field of nanomedicine: (1) they are readily biodegradable due to the relatively weak metal–ligand coordination bonds; (2) they are conducive to favourable loading efficiency of cargoes because of the high porosity and large pores; (3) they are easy to adjust, allowing for encapsulating or modifying diverse cargoes. Therefore, NMOFs have been widely explored for medical applications.

In this review, we focus on summarizing the nanomedical applications of NMOFs in the last few years, ranging from drug delivery to therapeutic agents (Fig. 1). Compared with the published overview articles, we categorize the delivered drugs according to their properties, highlight the advantages of MOFs in the delivery of various drug components, and pay more attention to the structural therapeutic components of MOFs in terms of treatment. By incorporating MOFs, our article covers a wider range of diseases, not limited to cancer. Moreover, we discuss the challenges and further development of NMOFs, in order to provide new insights and comprehensive understanding of NMOFs in nanomedical applications.

2. MOFs as delivery systems

MOFs, as an inorganic–organic hybrid nanocarrier, hold its intrinsic advantages over inorganic and organic carriers, owing

[a] *Institute for Regenerative Medicine, Shanghai East Hospital, School of Medicine, Tongji University, Shanghai 200092, China. E-mail: wenjunle@tongji.edu.cn, yihuihu2020@163.com*

[b] *Department of Cardiovascular Surgery, Shanghai East Hospital, School of Medicine, Tongji University, Shanghai 200092, China*

[c] *Shanghai Heart Failure Research Center, Shanghai East Hospital, School of Medicine, Tongji University, Shanghai 200092, China*

[d] *Shanghai East Hospital, Jinzhou Medical University, Jinzhou 121001, China*

† These authors contributed equally to this work.

This journal is © The Royal Society of Chemistry 2023

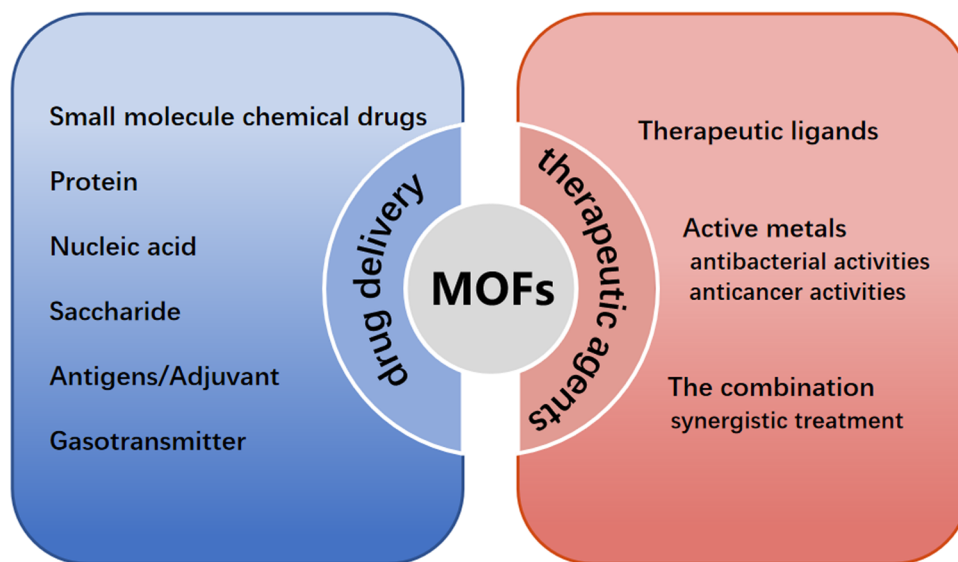*J. Mater. Chem. B*, 2023, **11**, 3273-3294 | **3273**

Fig. 1 Schematic diagram of the transportation and therapeutic effects of nanoscale MOFs–based materials.

to its high loading capacity and great biodegradability. Therefore, MOFs could be regarded as a promising candidate for further development of carriers to deliver therapeutic agents, ranging from small molecule drugs to biomacromolecules, such as chemical drugs, proteins, nucleic acids, saccharides, antigens, adjuvants, and gasotransmitters.

2.1. Small molecule chemical drugs delivery

2.1.1. Delivery and sustained release. Materials of institut lavoisier (MIL) family were the first to be investigated as drug delivery systems by the seminal work from Férey and coworkers as early as in 2006.[9] They synthesized two MIL-based (MIL-100 and MIL-101) nanocarriers for encapsulation of hydrophobic drugs, which were built from Cr^{3+} ions and trimesic acid (MIL-100) or terephthalic acid (MIL-101). Of note, the as-prepared MILs with giant pores allowed the drugs entrance, the unprecedented surface areas enabled high drug loadings, and the good water stability avoided rapid drug release. Ibuprofen as a

model drug has been successfully encapsulated into Cr-based MIL *via* simple impregnation method and achieved drug loadings up to 1.4 g ibuprofen/g MIL-101 (Cr). Nevertheless, the small dimensions of the pentagonal windows of MIL-100 (Cr) were close to the size of ibuprofen. Thus limited to valuable access, only 0.35 g ibuprofen was obtained per gram of MIL-100 (Cr). As shown in Fig. 2, the release kinetics of ibuprofen demonstrated that the drug release rate was slow, taking as long as 6 days for MIL-101 (Cr) and 3 days for MIL-100 (Cr) to release ibuprofen completely. However, because of the high toxicity of chromium, these MOFs were unsuitable for biomedicine applications, especially in the clinic. Consequently, less-toxic analogs, such as MIL (Fe) and MIL (Al), were developed for drug delivery and sustained release as biocompatible alternatives.[10–21]

Since then, many MOFs have been used as nanocarriers or intelligent carriers for the sustained and controlled release of drugs, as shown in Table 1. Up until now, MOFs have gained

Fig. 2 MIL family materials as drug delivery systems that slowly released ibuprofen. (A) 3D representation of MIL-101 (Cr) and MIL-100 (Cr). (B) Ibuprofen delivery from MIL-101 (Cr) and MIL-100 (Cr).[9] Copyright 2006, *Angewandte Chemie International Edition*.

3274 | *J. Mater. Chem. B*, 2023, **11**, 3273–3294

This journal is © The Royal Society of Chemistry 2023

Journal of Materials Chemistry B

Table 1 Summary of MOF-based nanocarriers for release behaviors

MOF-based nanocarriers	Drug	Loading capacity [wt%]	Release behaviour	Ref.
MIL-100 (Cr)	Ibuprofen	25.8	Sustained release 3 days	9
MIL-101 (Cr)	Ibuprofen	58	Sustained release 6 days	
MIL-53(Cr)	Ibuprofen	19.0	Sustained release 21 days	10
MIL-53(Fe)	Ibuprofen	17.5	Sustained release 21 days	
MIL-101 (Fe)	Cisplatin prodrug	12.8	Sustained release 3 days	42
	Cidofovir	42	—	14
	Azidothymidine triphosphate	42	—	
	Azidothymidine triphosphate	21	Sustained release 3 days	12
	Cidofovir	29	Sustained release 5 days	
	Doxorubicin	9	Sustained release 14 days	
	Flurbiprofen	37	Sustained release 72 hours	18
	Indocyanine green	16.9	Sustained release	20
MIL-101 (Al)	Indocyanine green	18.2	Sustained release	
MIL-88 (Fe)	Indocyanine green	10.6	Sustained release	
MIL-88A	Busulfan	8	Sustained release	13
MIL-89	Busulfan	10	Sustained release	
MIL-100	Busulfan	26	Sustained release 24 hours	
MIL-53	Busulfan	14	Sustained release 24 hours	13
	Flurbiprofen	20	Sustained release 72 hours	18
	Vancomycin	11.5	Sustained release	21
MIL-100	TPT	11.6	Photon-induced release	36
	[Ru(pcymene)Cl$_2$(pta)]	—	Sustained release	15
	Caffeine	42	Sustained release 48 hours	16
	Phosphated gemcitabin	30	Sustained release 24 hours	17
	Flurbiprofen	46	Sustained release 72 hours	18
	Gemcitabine monophosphate	30	pH-Responsive release	19
Ca-MOF	Flurbiprofen	10	Sustained release 72 hours	18
MOF-5	5-FU	84.1	pH-Responsive release	43
Fe$_3$O$_4$ nanorods@HKUST-1	NIM	16.7	Sustained release 11 days	29
HKUST-1	5-FU	40.2	Sustained release 96 hours	44
ZIF-8	5-FU	39.8	pH-Responsive release	32,45
	Doxorubicin	4.67	Sustained release 30 days	46
		20	pH-Responsive release	47
	Curcumin	12.7	pH-Responsive release	48
	Curcumin	3.4	pH-Responsive release	49
	Verapamil hydrochloride	32.0	pH-Responsive release	50
	Doxorubicin	8.9		
	3-Methyladenine	19.8	pH-Responsive release	51
	Chloroquine diphosphate	18.0	pH-Responsive release	52
	Cytarabine-IR820	39.8	pH-Responsive release	40
	Tetracycline	59.7	pH-Responsive release	53
ZIF-90	Doxorubicin	13.5	Sustained release 18 hours	54
	5-FU	36.4	Sustained release 25 hours	
Zn-cpon-1	5-FU	44.7	pH and temperature dual-triggered release	55
	6-Mercaptopurine	4.8		
Zn$_8$(O)$_2$(CDDB)$_6$(DMF)$_4$(H$_2$O)	5-FU	53.3	Sustained release 72 hours	56
Cu-BTC MOF	5-FU	8.2	Sustained release 2 days	57
Cu$_2$(COO)$_4$(H$_2$O)$_2$	Ibuprofen	45	Sustained release 96 hours	58
	Guaiacol	62	Sustained release 48 hours	
	Anethole	60	Sustained release 3.5 hours	
mesoMOFs	Doxorubicin	55	Sustained release 72 hours	59
MOF-74 (Fe)	Ibuprofen	15.9	Anion-exchange controlled release	60
Gd-pDBI	Doxorubicin	12	pH-Response release	61
UiO-66	Cisplatin prodrug	12.3	Sustained release 8 hours	23
	Alendronate	51.4	pH-Response release	24
	5-FU	—	Zn^{2+} or thermal-triggered release	25
	Taxol	14	Sustained release 300 hours	26
	Cisplatin	4.8		
	Dichloroacetic acid	13.7	pH-Response release	27
	Dichloroacetate	20.7	Sustained release	28
UiO-67	Taxol	10	Sustained release 300 hours	26
	Cisplatin	1		
ZJU-800	Diclofenac sodium	58.8	Pressure-controlled release	62
ZJU-64	MTX	13.45	Sustained release 72 hours	63
ZJU-101	Diclofenac sodium	54.6	pH-Responsive release	64
NU-901	α-Cyano-4-hydroxycinnamic acid	79.0	Sustained release 30 days	65
NU-1000	α-Cyano-4 hydroxycinnamic acid	81.0		
Bio-MOF-1	Procainamide	22	Cation-triggered release	11
Bio-MOF-Zn	Diclofenac sodium	172	Sustained release 48 hours	66

This journal is © The Royal Society of Chemistry 2023

J. Mater. Chem. B, 2023, **11**, 3273–3294 | **3275**

Table 1 (*continued*)

MOF-based nanocarriers	Drug	Loading capacity [wt%]	Release behaviour	Ref.
ZFH-DGR	Dox	5.4 ± 0.1	pH-Responsive release	41
	FITC-OVA	6.9 ± 0.1		
UMCM-1	Doxorubicin	—	pH- or competitive binding agent-triggered release	67
IRMOF-74	Gemcitabine	113	Sustained release	68
IRMOF-3	5-FU	20.4	Sustained release 96 hours	69
	Celecoxib	26.4	pH-Responsive release	70
	Doxorubicin	46.8		
MOF-In1	5-FU	34.3	Zn^{2+}-triggered release	71
γ-CD-MOF	Captopril	19.3	Sustained release	72
	Ibuprofen	26	Sustained release	73
	Ibuprofen	12	Sustained release 48 hours	74
	Lansoprazole	9.4		
α-CD-MOF	5-FU	25.7	Sustained release 36 hours	75

great success in the delivery of active pharmaceutical ingredients (API) and prodrugs, including MIL, zeolitic imidazolate framework (ZIF), porous coordination network (PCN), university of oslo (UiO), isoreticular metal-organic framework (IRMOF), biomolecule-based MOFs (bio-MOFs) and cyclodextrin (CD)-based MOFs. These MOFs are superior to other delivery materials in protecting drugs from degradation, precise delivery, and controllable release.

Among tens of thousands of known MOFs, UiO-66 constructed from zirconium(IV) oxoclusters and terephthalate anions, possessed high stability and porosity as one of the most promising nanocarriers for drug delivery. Furthermore, it is more feasible to modify functional groups on UiO-66, so that both hydrophilic and hydrophobic drugs can be encapsulated through reasonable functionalization. For example, Serre and coworkers explored the relationships between drug encapsulation performances and the functionalized organic linker of UiO-66.[22] It was first demonstrated that polar or apolar functional groups on UiO-66 exhibited different drug payloads, in which it appeared that the large octanol-water partition coefficient and low hydrogen bond functional groups were conducive to loading amphiphilic cosmetic caffeine, whereas the loading of the hydrophobic drug ibuprofen was enhanced with large solvent surface and free volume functional groups. It highlighted that the competition between the adsorption of the solvent and the drug during the encapsulation process played a crucial role.

In 2014, Lin and his group first used UiO with hexagonal-plate morphologies for the co-delivery of cisplatin prodrug and small interfering RNAs (siRNAs) *via* encapsulation and surface coordination to enhance therapeutic efficacy in drug-resistant ovarian cancer cells.[23] As shown in Fig. 3, UiO with high porosity allows the cisplatin prodrugs to encapsulate into the channels and metal sites on the surfaces to enable the phosphate group to coordinate binding with siRNA. UiO could effectively protect siRNA from degradation by nuclease, exhibited multiple therapeutics for drug-resistant cancer therapy, and represented a unique nanocarrier platform for co-delivery. Afterwards, UiO-based platforms (*i.e.*, UiO-66, UiO-67) were also been utilized to deliver various chemical drugs, such as 5-FU, taxol, cisplatin, and dichloroacetate, to defeat tumors.[24–28] On the one hand, UIO kept the structure and efficacy of anticancer drugs intact; on the other hand, the high porosity of UIO boosted drug loading capacity and achieved better anticancer effects.
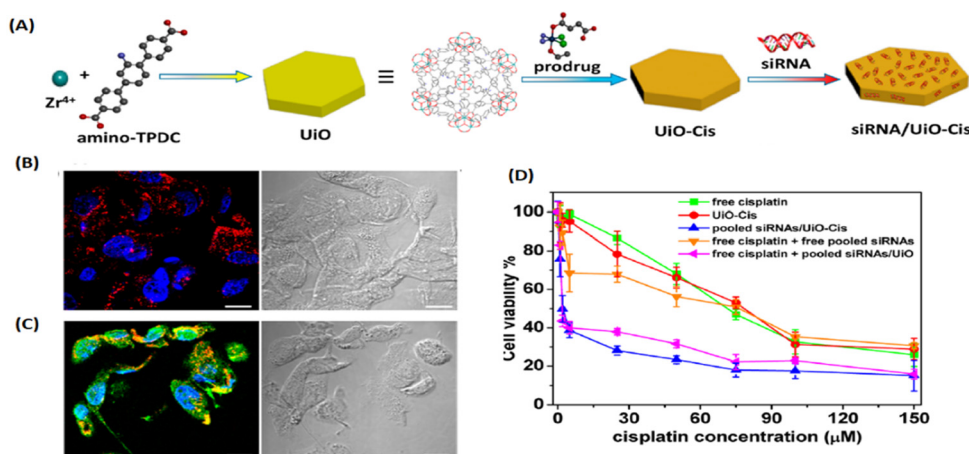

Fig. 3 UIO as a unique co-delivery platform. (A) Schematic presentation of siRNA/UiO-Cis synthesis and drug loading; (B) CLSM images showing cell apoptosis and siRNA (TAMRA-labelled, red) internalization in SKOV-3 cells after incubation with siRNA/UiO; and (C) siRNA/UiO-Cis for 24 h; (D) SKOV-3 cells were incubated with free cisplatin, UiO-Cis, pooled siRNAs/UiO-Cis, free cisplatin plus free pooled siRNAs, and free cisplatin plus pooled siRNAs/UiO at different concentrations for 72 h, and then the cytotoxicity was determined by MTT assay.[23] Copyright 2014, *Journal of the American Chemical Society*.
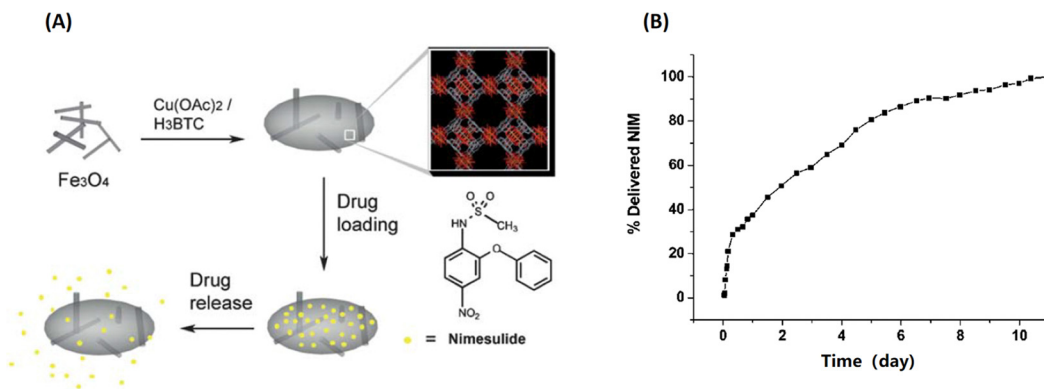
3276 | *J. Mater. Chem. B*, 2023, 11, 3273–3294

This journal is © The Royal Society of Chemistry 2023

Fig. 4 Fe_3O_4@MOF for magnetic targeted drug delivery and controlled release. (A) The synthesis and action of $Fe_3O_4/Cu_3(BTC)_2$ nanocomposites for potential targeted drug release; (B) the NIM release process in physiological saline at 37 °C.[29] Copyright 2011, *Journal of Materials Chemistry*.

2.1.2. Targeted delivery. Targeted drug delivery systems could not only reduce the side effects, but also improve the therapeutic efficacy. Due to the rich physicochemical surface of MOFs, it enabled targeting agents to decorate onto MOFs for targeted delivery. Unfortunately, the architectures of some MOFs may be prone to disintegration during the process of drug delivery, making them ineffective for targeted or even non-targeted delivery. Consequently, it is essential to develop and select MOFs that are stable under physiological conditions, and could be degraded at the site of lesions for drug delivery.

Zhang *et al.* firstly fabricated MOF-based nanocomposites (named Fe_3O_4 nanorods@HKUST-1) for magnetic targeted drug delivery.[29] As shown in Fig. 4, the magnetic MOF nanocomposites were obtained by incorporating Fe_3O_4 nanorods into 3D HKUST-1, conferring them excellent candidates for magnetic targeted drug delivery and controlled release. Then, Nimesulide (NIM), an anti-cancer drug for pancreatic cancer treatment, was laden into Fe_3O_4 nanorods@HKUST-1. There were up to 0.2 g NIM adsorbed per gram Fe_3O_4 nanorods@HKUST-1 composite. Interestingly, it took as long as 11 days for NIM release in physiological saline at 37 °C. Importantly, a variety of

conjugation methods have been developed to attach functional moieties to MOFs.[30]

Therefore, covalent attachment targeting cargoes onto MOFs is another important approach for targeted delivery. For example, Dong and coworkers designed and developed a folic acid (FA)-targeting bearing UiO-based drug delivery platform (Fig. 5(A)). The doxorubicin (DOX)-loaded Mi-UiO-68 was covalently modified with FA targeting agent (DOX@UiO-68-FA) *via* thiol-maleimide Michael-type addition for highly effective hepatoma therapy. Compared with free DOX and DOX@Mi-UiO-68, DOX@Mi-UiO-68-FA possessed the best therapeutic effect.[31] As shown in Fig. 5(B), Forgan *et al.* reported three surface modification protocols, including coordination modulation, postsynthetic exchange and covalent click modulation, to attach biomolecules (*i.e.*, FA, biotin, PEG) on the surface of UiO-66 for dichloroacetic acid (DCA) targeting delivery. They not only demonstrated that biomolecule functionalization could improve the properties of UiO-66, but also confirmed that the therapeutic efficiency was drastically enhanced with a 300-fold increase in the selective cytotoxicity of DCA@UiO-66-FA toward the overexpression of FR of cancer cells.[28]
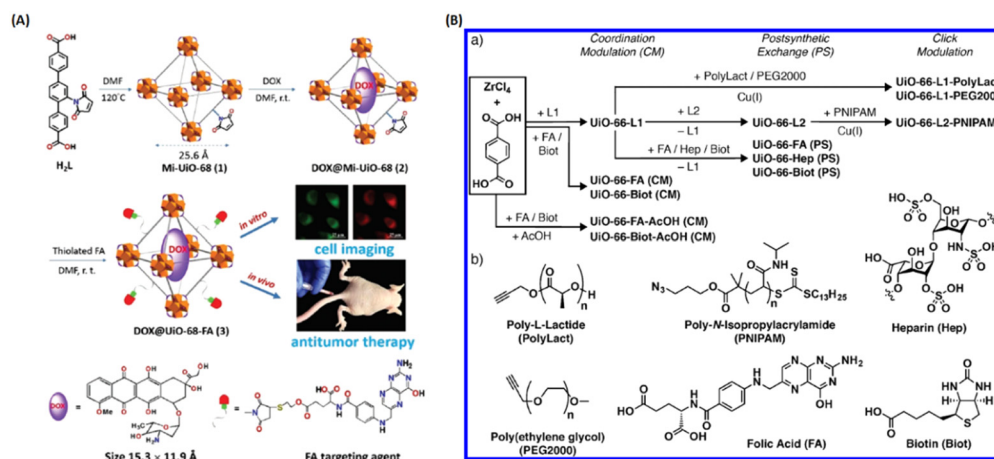

Fig. 5 Covalent attachment of targeting agents to MOFs for targeted delivery. (A) Design and fabrication of FA targeting agent-decorated drug delivery system and its application in cell imaging and *in vivo* antitumor therapy.[31] Copyright 2016, Chemical Communications (Camb). (B) Synthetic scheme for the three surface-modified protocol of UiO-66 and the attachment of chemical structures.[28] Copyright 2018, *ACS Applied Materials & Interfaces*.

This journal is © The Royal Society of Chemistry 2023

J. Mater. Chem. B, 2023, **11**, 3273–3294 | **3277**

Fig. 6 ZIF-8 as a pH-sensitive delivery vehicle for the controlled release of 5-fluorouracil (5-FU). (A) The scheme of pH-response of the encapsulated 5-Fu release from ZIF-8; (B) the NIM release process in physiological saline at 37 °C.[32] Copyright 2014, *Dalton Transactions*.

2.1.3. Stimuli-triggered release. Nowadays, stimuli-responsive cargo vehicles are popular for controllable drug release, including tumor microenvironment (TME)-trigger and external-trigger. In 2012, Wang and coworkers reported ZIF-8 as an efficient pH-sensitive drug delivery vehicle for the controlled release of 5-fluorouracil (5-FU).[32] As shown in Fig. 6, the ZIF-8 degraded under acidic condition and thus released 5-FU for therapy. The release profiles showed that 5-FU was released much faster in mild acidic buffer solution (pH 5.0) than at a neutral pH of 7.4. Since then, ZIF-based MOFs (ZIF-8, ZIF-90, *etc.*) have been widely used for the incorporation of diverse drugs and imaging agents for pH-responsive release.[33–35] Furthermore, external (*i.e.*, light, temperature, ions)-triggered drug release has also received much attention. As shown in Fig. 7, the Gref team achieved light-triggered drug delivery by encapsulating topotecan (TPT) in MIL-100.[36] TPT monomers aggregated within MIL-100 and stabilized the 3D structure as a

''ship in a bottle'', avoiding the ''burst'' release. However, one-and two-photon light irradiation could promote TPT release from MIL-100. Sada and coworkers constructed a smart MOF for thermal on–off controllable release by modification with a thermoresponsive polymer (PNIPAM) on UiO-66 (UiO-66-PNIPAM) *via* surface post-synthetic modification techniques.[37] Guest molecules, such as resorufin, caffeine and procainamide, were rapidly released at a low temperature (25 °C) and suppressed release at a high temperature (40 °C) through the conformational change of PNIPAM. By modifying carboxylato-pillar[5]arene (CP5)-based supramolecular switches onto the surface of UiO-66, Yang *et al.* constructed a superior Zn^{2+} and thermal dual stimuli-triggered drug release nanoplatform (UiO-66-NH-Q-CP5).[25] On the one hand, Zn^{2+} has a higher binding affinity toward CP5, and induced dethreading of the CP5 rings from the Q stalks to release 5-FU from the pores of UiO-66. On the other hand, the supramolecular interactions between the

Fig. 7 MIL-100 as a light triggered delivery system for transporting topotecan (TPT). (A) Schematic representation of one- or two-photon photodelivery of TPT from MIL-100.[36] Copyright 2014, Journal of Medicinal Chemistry. (B) Schematic representation of the thermoresponsive controlled release from UiO-66-PNIPAM.[37] Copyright 2015, Chemical Communications (Camb). (C) Schematic representation of the stimuli-responsive mechanized UiO-66-NH_2 MOFs equipped with positive charged quaternary ammonium salt (Q) encircled by pillarene[2]pseudorotaxanes. The mechanized nanoUiO-66-NH2 MOFs can be operated either by thermal heating or by Zn^{2+} competitive binding in regulation of the release of cargo molecules.[25] Copyright 2015, *Small*.
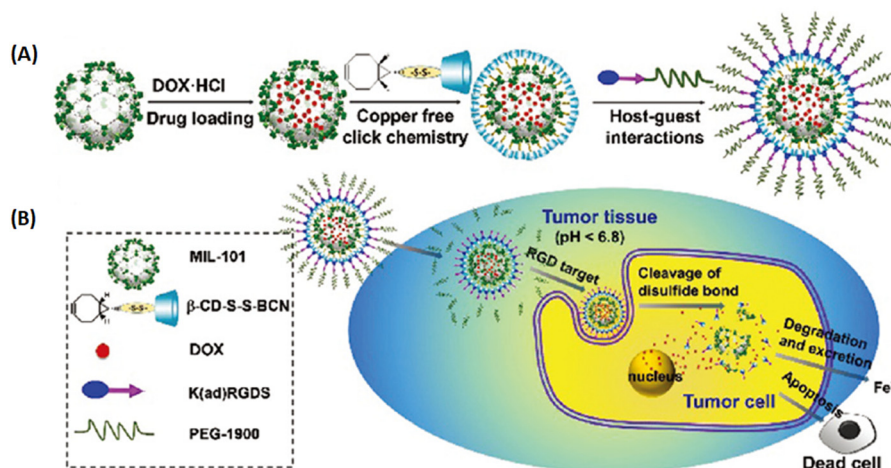
Fig. 8   MIL-101 as a multifunctional drug delivery system for targeting and pH/GSH dual-responsive release. (A) Schematic illustration of drug loading and post-synthetic modification procedure, and (B) the tumor-targeting drug delivery and cancer therapy procedure of the multifunctional MOF based DDS.[39] Copyright 2015, *Nanoscale*.

CP5 rings and the Q stalks are weakened by increasing temperature, which also led to the gradual release of 5-FU. In follow-up work, they further designed a multi-stimulus (pH, Ca^{2+}, thermal) responsive UiO-66-based nanocarrier with gated scaffolds to control drug release for anticancer therapy.[38]

2.1.4.   Combination of targeted delivery and stimulus-triggered release. The combination of targeted delivery and stimulus-triggered release could be a desirable drug delivery system for precise therapy. Due to the high drug loading and available surface modification, MOFs have become a promising candidate for precise drug delivery. Zhang and coworkers developed a MIL-101-based tumor targeting and dual-responsive multifunctional drug delivery system by two-step surface modification.[39] As shown in Fig. 8, after loading doxorubicin hydrochloride (DOX·HCl), MIL-101-N_3 was modified with bicyclononyne functionalized β-cyclodextrin derivative (β-CD-SS-BCN) through strain-promoted [3+2] azide-alkyne cycloaddition, and the disulfide bond was introduced for redox responsiveness. Then, by taking advantage of the host–guest interaction between β-CD and adamantane to modify the functional polymer, this polymer was functionalized with $\alpha_v\beta_3$ integrin to target peptide (RGD) and PEG chains *via* pH responsive benzoic imine bond. Therefore, the multifunctional drug delivery system exhibited tumor targeting to improve tumor accumulation and enhance cellular uptake by dissociating the benzoic-imine bond between PEG and RGD peptide in an acidic environment. Intracellular GSH cleaved the disulfide bond between β-CD and MIL-101 to open the channel, and release drugs for effective inhibiting tumor growth with minimal side effects. Luan *et al.* proposed a versatile strategy to load drugs/prodrugs into ZIF-8, and functionalize hyaluronic acid (HA) on the surface of ZIF-8 for tumor-targeted delivery and pH-triggered release for chemo-photothermal therapy.[40] Since the drug cytarabine (Ara) cannot be encapsulated into ZIF-8 satisfactorily, indocyanine green (IR820) was utilized to bond with Ara for the formation of prodrug (Ara-IR820) for efficient encapsulation, in which sulfonic groups of the prodrug strengthen the interaction between Ara-IR820 and ZIF-8. The obtained HA/Ara-IR820@ZIF-8 displayed excellent therapy with HA-based targeted and ZIF-8-based pH-responsive release. Moreover, Ara-IR820 endowed the delivery system with unique fluorescence-imaging-guided chemo-photothermal therapy of tumors.

2.1.5.   Bio-MOFs. For the abovementioned MOFs, it is possible to leach toxic metal ions or harmful constituents during delivery. So, some green MOF-based carriers have been developed, called bio-MOFs, which are constructed from bio-molecular building blocks (*i.e.*, amino acids, nucleobases) and bimetallic ions (*i.e.*, Zn^{2+}, Ca^{2+}). Rosi and his colleagues firstly synthesized porous bio-MOF-1, which is composited by adenine and Zn^{2+}. Furthermore, they exploited bio-MOF-1 for storage of the cationic drug procainamide and cation-triggered drug release by cation-exchange.[11] We also developed a facile one-pot strategy to construct peptide-doped bio-MOF, denoted as ZFH-DGR, which was built by Fmoc-His, targeting peptide Fmoc-HDGR and Zn^{2+}, as shown in Fig. 9.[41] The as-prepared bio-MOF can encapsulate hydrophobic chemotherapy drugs, hydrophilic proteins and nanomaterials (negatively charged gold nanoparticles, positively charged gold nanorods) for targeting delivery to the precise therapy of tumors.

2.2.   Protein delivery

It is well known that proteins are prone to deactivation by degradation, and most native proteins are membrane impermeable. So, it is crucial to develop carrier systems for the efficient delivery of functional proteins. Nowadays, there are three main approaches to fabricate MOF-based nanocarriers for protein protection/delivery, including encapsulation, covalent conjugation and protein/peptide as organic linkers, as shown in Table 2.

2.2.1.   Encapsulation approaches. In 2006, Balkus and co-workers firstly immobilized microperoxidase-11 (MP-11) in the

This journal is © The Royal Society of Chemistry 2023

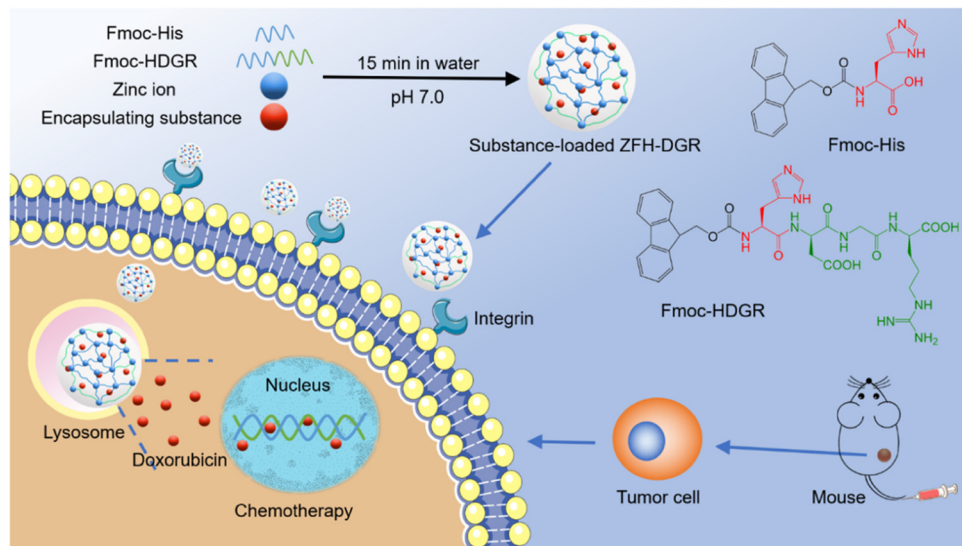*J. Mater. Chem. B*, 2023, **11**, 3273–3294 | **3279**

Fig. 9 Bio-MOFs construction from amino acids/peptides and bimetallic ions as green carriers for targeting delivery. One-pot construction of targeted bio-MOF/drugs and their targeted therapy.[41] Copyright 2021, *ACS Applied Materials & Interfaces*.

Table 2 Summary of MOF-based nanocarriers for protein delivery methods

MOFs	Proteins	Methods	Ref.
$[Cu(OOC–C_6H_4\text{-}C_6H_4\text{–}COO).^{1/2} C_6H_{12}N_2]_n$ MOF	MP-11	Immersed method	76
Tb-mesoMOF	MP-11	Immersed method	77,95
Tb-mesoMOF	Myoglobin	Immersed method	96
Tb-mesoMOF	Cyt *c*	Immersed method	97
PCN-333	HRP, Cyt *c*, MP-11	Immersed method	88
ZIF-8	Cyt *c*, HRP, lipose	One-pot coprecipitation method	78
ZIF-10			
	Cyt *c*		
ZIF-90	Catalase	One-pot coprecipitation method	80
ZIF	Catalase	One-pot coprecipitation method	82
ZIF-8	GOx	One-pot coprecipitation method	86
ZIF-8	GOx&HRP	One-pot coprecipitation method	81
ZIF-8	BSA, β-Gal, HAS, caspase3, EGFP, RFP,	One-pot coprecipitation method	84
ZIF-8	BSA, Cyt *c*, geloion	One-pot coprecipitation method	85
ZIF-8	GOx&insulin	One-pot coprecipitation method	87
ZIF-8, HKUST-1, MIL-88A, Eu/Tb-BDC	BSA/HAS/OVA/lysozyme, HRP/ribonucleaseA/ haemoglobin/trypsin/lipase/insulin/glucose-dehydrogenase	Biomimetic mineralization	79
PCN-224	GOx&catalase	Immersed method	83
PCN-333	SOD&catalase	Immersed method	98
$[(Et_2NH_2)(In(pda)_2)]_n$, $[Zn(bpydc)(H_2O). (H_2O)]_n$, IRMOF-3	EPGF, CAL-B	Bioconjugation	89
MIL-88B-NH$_2$	Trypsin	Bioconjugation	90
CYCU-4	Trypsin-FITC	Vortex-assisted host–guest interaction	91
Zn-ferritin MOF	Ferritin	As modular component	93
Metal-ferritin MOFs	Ferritin	As modular component	94

3-dimensional (3D) $[Cu(OOC–C_6H_4–C_6H_4–COO)_{1/2}C_6H_{12}N_2]_n$ MOF by immersed method.[76] The MOF-supported MP-11 exhibited high catalytical activity and could be effectively resistant to organic solvents. Then, they further immobilized MP-11 into mesoporous Tb-TATB (denoted MP-11@Tb-mesoMOF), and evaluated the superior enzymatic catalysis performance with the recyclability and solvent adaptability of MP-11@Tb-mesoMOF.[77] Compared to mesoporous silica material MCM-41 adsorbed MP-11 (MP-11@MCM-41), MP-11@Tb-mesoMOF

presented higher catalytic activity due to the richness of the MOF structures, which opened a window towards immobilizing enzymes/proteins into MOFs. After that, researchers exploited the ever-expanding MOFs to immobilize various proteins for biomedical applications.

Taking advantage of the simple and friendly synthesis of ZIF, the Liu group developed a facile and general method for the one-pot synthesis of protein-embedded ZIF-8/10 by coprecipitation method.[78] As shown in Fig. 10, it demonstrated that

3280 | *J. Mater. Chem. B*, 2023, **11**, 3273–3294

This journal is © The Royal Society of Chemistry 2023

Fig. 10 ZIF-8 for enzymes and functional proteins delivery. (A) Preparation of the Cyt c-embedded ZIF-8 and its biocatalysis. (B) The relative peroxidase activity of Cyt c, Cyt c/ZIF-8 composite, PVP/Cyt c mixture, Cyt c/zinc ion mixture, Cyt c/2-methylimidazole mixture, and Cyt c/ZIF-8 mixture.[78] Copyright 2014, *Nano Letters*.

the peroxidase activity of cytochrome c (Cyt c)-embedded in ZIF-8 increased 10-fold compared to free Cyt c in solution. Following up on this work, it was a rapid development of ZIF-encapsulated enzymes and functional proteins for pH-responsive delivery or co-delivery in imaging and therapy applications.[79–87] Afterwards, Zhou and coworkers rationally designed ultra-large mesoporous cages of PCN-332/333 and developed single-enzyme encapsulation (SEE).[88] The size of the cage could be larger than the enzyme, but cannot accommodate two enzymes due to size limitation, for the encapsulation of a single-enzyme molecule in one cage. Thus, the SEE could effectively prevent enzyme aggregation and denaturation.

2.2.2. Covalent conjugation approaches. The functional groups of the organic linkers on the surface of MOFs are available for post-synthetic modification, which allowed proteins to decorate onto MOFs via bioconjugation. As shown in Fig. 11, by using carboxylate or amino groups on the surface of MOFs, the team of Park and Lin successfully achieved enhanced green fluorescent protein (EGFP)-, candida antarctica lipase B (CAL-B) and trypsin-functionalized MOFs with different structural architectures by covalent conjugation of $-NH_2$

and $-COOH$.[89,90] Lin and coworkers developed a "green" technique of protein-immobilized MOFs bioreactor (trypsin-FITC@CYCU-4) via vortex-assisted host–guest interaction.[91] They found that CYCU-4 with large channels (larger than 1.4 nm) could capture FITC dye to their pores through strong π–π interaction and hydrogen bonding between the organic linker and FITC. Thus, the orientation of FITC-tagged trypsin was immobilized on CYCU-4 by a very efficient host–guest interaction, which exhibited commendable biocatalytic performance.

2.2.3. Proteins as organic linkers. The construction of metal–peptide/protein frameworks is a robust approach for delivering peptides or proteins. Rosseinsky et al. firstly reported MOFs that consist of dipeptides or multiple-peptide coordinated to Zn^{2+} ions, and found that the exchange of amino acids can radically alter the structure and function of MOF.[92] As shown in Fig. 12, Tezcan and colleagues constructed a 3D metal-protein framework that was formed by ferritin with Zn coordination via a ditopic benzene-dihydroxamate linker.[93] Furthermore, they established a large library of metal–ferritin MOFs through 3 different metallo-ferritin nodes and 5 organic
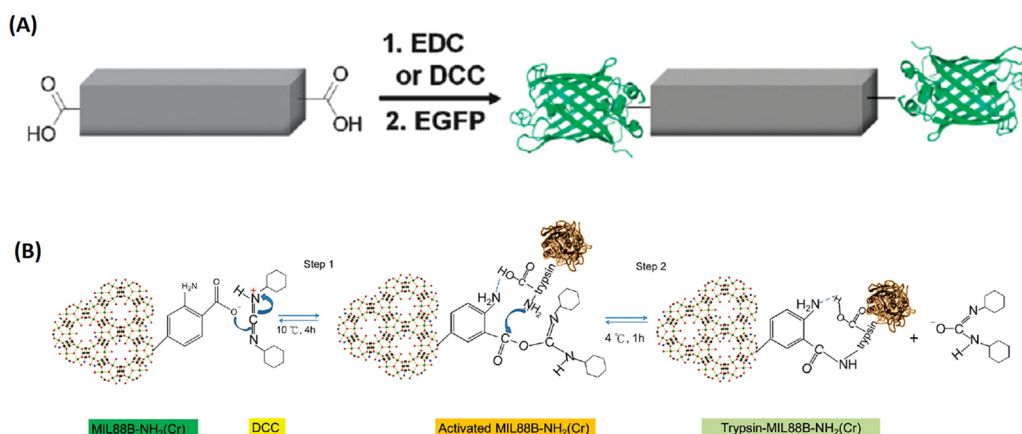

Fig. 11 The bioconjugation of proteins onto the surface of MOFs via functional groups of the organic linkers. (A) The bioconjugation of the 1D-MOFs, $[(Et_2NH_2)(In(pda)_2)]_n$ with EGFP.[89] Copyright 2011, Chemical Communications (Camb). (B) Trypsin immobilization onto DCC-activated MIL-88B-NH2.[90] Copyright 2012, *ChemPlusChem*.

Fig. 12 Metal–peptide/protein frameworks as robust vehicles to deliver peptides or proteins. (A) Scheme for metal/linker-directed self-assembly of ferritin into 3D crystals.[93] Copyright 2015, *Journal of The American Chemical Society*. (B) The construction of a library of 3D ferritin-MOFs with different modular components.[94] Copyright 2017, *Journal of The American Chemical Society*.

linkers with hydroxamate head groups.[94] These demonstrated that the self-assembly of ferritin-MOFs is highly robust and displays dynamic behavior.

2.3. Nucleic acid delivery

It is crucial to develop non-viral vectors for nucleic acid delivery, which can promote applications in the field of gene therapy and gene editing. MOFs, as novel carriers, play vital roles in nucleotide delivery. Nucleic acid with some intrinsic advantages, such as excellent biocompatibility, high electronegativity, multiple functional groups, *etc.*, which enabled MOFs to load nucleic acid with various methods, ranging from adsorption, encapsulation and covalent attachment to as building blocks.[99]

Nucleic acids with rich structure and multiple functional groups could sever as organic linkers to coordinate with metal ions, forming supramolecular networks. Kimizuka *et al.* reported on the supramolecular networks self-assembled from nucleotide (5′-AMP, 5′-GMP, 5′-UMP, 5′-CMP) and lanthanide ions, which can even encapsulate fluorescent dyes, proteins, drugs or nanoparticles for biomedical applications.[100]

Later, Zhou and colleagues synthesized two nucleobase-incorporated MOFs (PCN-530 and TMOP-1) by introducing adenine as co-ligand.[101] Gref and coworkers explored the impact of phosphate groups on nucleoside analogue drugs (*i.e.*, azidothymidine and its phosphorylated derivatives) of loading capacity, and demonstrated that the interaction between drugs' phosphate groups and the Lewis iron(III) acid site from MIL-100(Fe) increased encapsulation efficiency.[102] Inspired by this, Liu *et al.* synthesized Se/Ru@MIL-101 composite to load siRNAs *via* surface coordination between the unsaturated Fe(III) sites of MIL-101 and phosphate residues

on the backbone of siRNA, for delivery of siRNAs to reverse multidrug resistance therapy.[103]

The research team of Mirkin constructed UiO-66-nucleic acid conjugates through click reaction, which exhibited increased stability and enhanced cellular uptake.[104] UiO-66-N_3 were synthesized by 2-azidoterephthalic acid and $ZrOCl_2 \cdot 8H_2O$ *via* solvothermal reaction, and then dibenzylcyclooctyne-functionalized DNA reacted with the –N_3 group of UiO-66 to obtain DNA-UiO-66. Wang *et al.* developed a versatile nanosystem (Ce6-DNAzyme@ZIF-8) by encapsulating a therapeutic DNAzyme agent into ZIF-8 for self-sufficient gene therapy and photodynamic therapy (PDT).[105] The as-prepared Ce6-DNAzyme@ZIF-8 exhibited efficient intracellular delivery and pH-responsive release of Ce6-DNAzyme, and Zn^{2+} ions as co-factor concomitantly supplied to boost gene therapy, along with Ce6-based PDT. Zhou *et al.* tuned the pore size of IRMOF-74 with different organic linkers to precisely include different lengths of ssDNA.[106] IRMOF-74 can protect ssDNA excellently, because the entire nucleic acid completely confining inside the pores, and exhibited high transfection efficiency in immune cells.

2.4. Antigens/adjuvant delivery

Tumor vaccines, consisting of antigen and adjuvant, have been considered as a promising therapy. Therefore, nanocarrier delivery systems afford benefits for promoting the development of vaccines. As a well-known class of porous hybrids, MOFs have been used as carriers to stimulate the development of vaccines for tumor therapy.

As shown in Fig. 13, Qu *et al.* developed a ZIF-8-based vaccine by *in situ* encapsulating ovalbumin (OVA) antigens and absorbing unmethylated cytosine-phosphate-guanine oligodexynucleotides (CpG ODNs) adjuvants, donated as OVA@ZIF-8-CpG.[107] The obtained vaccines have good biocompatibility and are pH-responsive to the delivery of OVA and CpG ODNs into the same

Fig. 13 MOFs used for co-delivery of antigens and adjuvants to construct tumor vaccines. (A) The preparation of the OVA@ZIF-8-CpG vaccine. (B) The use of the OVA@ZIF-8-CpG vaccine to induce a humoral and cellular immunity response.[107] Copyright 2016, *Advanced Functional Materials*.

antigen presenting cells (APCs) efficiently, which induced a strong systemic immune and potent immune memory response. Zhang's research group also fabricated OVA and CpG codelivery based on pH-responsive MOFs nanocarrier for enhanced cancer immunotherapy.[108] Similar with proteins and nucleic acids delivery, MOFs could be applied to the delivery of antigens/adjuvants for enhanced immune and synergistic therapy.[109–112]

2.5. Gasotransmitter delivery

Recently, gasotransmitter-based therapy has attracted tremendous attention, such as nitric oxide (NO), carbon monoxide (CO), hydrogen sulfide (H_2S), and hydrogen (H_2). It is vital to develop gas releasing systems because of their short half-life. MOFs, a "star" hybrid, hold great promise for gas storage and delivery in biological applications.

Morris *et al.* found that NO and H_2 have relatively weak interaction with metals in HKUST-1, which is an advantage for gas delivery.[113] In particular, the adsorption capacity of NO on HKUST-1 is significantly high, and is enough to be biologically active and inhibit platelet aggregation. Based on gas–metal interaction, they further developed CPO-27, MIL-88(Fe), Ca-MOF, *etc.* to store and deliver NO or H_2S for potential biomedical applications.[114–117] Metzler-Nolte and coworkers prepared high-quality MIL-88B-Fe and NH_2-MIL-88B-Fe with a large number of unsaturated metal sites for loading and delivery CO.[118] CO was captured by the iron unsaturated coordination site of MIL-88, and released during the decomposition.

Gas-releasing molecules were recently developed for controllable release, such as NO donors and CO donors. Diazeniumdiolate is attractive for NO release and can be facilitated to modify nanomaterials through the reaction of the amine with NO/NO_2^- to form N-nitrosamine. Based on this, NO donor-modified MOFs were developed by covalent modification for controlled release of NO.[119–121] A few research groups constructed stimulus-responsive CO-releasing MOFs by using the open 2,2′-bipyridine (bpy) centers in MOFs (UiO-67-bpy,

UiO-66-BDP, Ti-MOFs) to coordinate with CO donors ($MnBr(CO)_5$), leading to the formation of $MnBr(bpydc)(CO)_3$@MOFs.[122–124] They achieved efficient and controllable CO release by light-/H_2O_2-triggered therapy. Additionally, Furukawa and coworkers used 2-nitroimidazole and 5-methyl-4-nitroimidazole as organic ligands to construct NO-based ZIFs, and achieved precisely controlled NO release *via* two-photo laser activation.[125]

2.6. Saccharide delivery

Heparin, a linear glycosaminoglycan, has been extensively used as an anticoagulant. Pidko and coworkers synthesized a *de novo* heparin-MIL-101(Fe) composite with excellent biocompatibility and pronounced anticoagulant activity. Furthermore, they used the as-prepared heparin-MIL-101(Fe) as a drug-releasing depot to coat on the structure of streptokinase (SK)-entrapped alumina, named as Hep-MIL-101(Fe) + SK@alumina, which was applied on polytetrafluoroethylene vein implants.[126]

3. MOFs as therapeutic agents

Some therapeutic drugs with several functional groups make them possible to directly construct MOFs as bridging ligands, or biologically active cations as central metal ions or even their combinations could build therapeutic MOFs for biomedical applications.

3.1. Therapeutic ligands

Therapeutic ligands, as linkers to construct nanoscale coordination polymers (NCPs) or MOFs, afford high atomic economy to generate high drug capacity and avoid the toxicity of exotic organic ligands. Therefore, it is a judicious approach to develop therapeutic MOFs for broadening applications.

As early as 2005, Li *et al.* synthesized a 2D coordination polymer, which was self-assembled from enoxacin and Mn^{2+} ions through covalent coordination and hydrogen bonds under hydrothermal conditions.[127] However, a majority of drugs or

This journal is © The Royal Society of Chemistry 2023
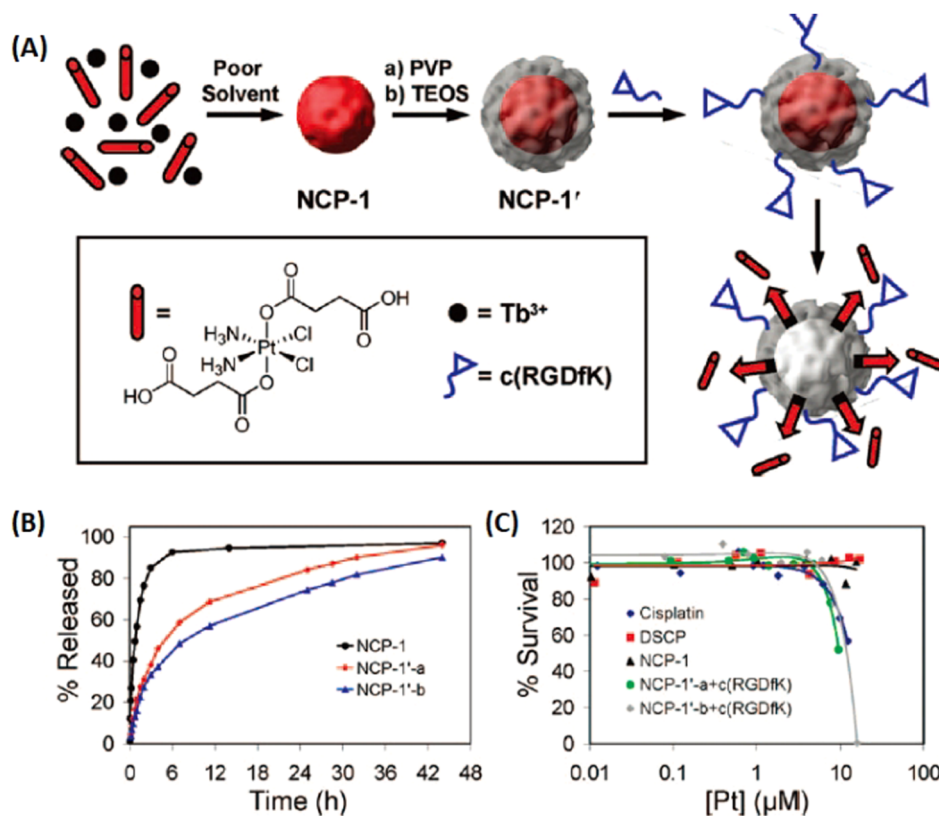
J. Mater. Chem. B, 2023, **11**, 3273–3294 | **3283**

Fig. 14 Cisplatin-based prodrug as organic linkers to construct NCPs for the controllable release of the Pt species. (A) The preparation of NCPs; (B) the Pt release from NCPs against time; (C) cytotoxicity assay for HT-29 cells against Pt concentration of NCPs.[128] Copyright 2008, *Journal of the American Chemical Society*.

prodrugs lacked molecular rigidity and were unstable in high temperatures/pressures conditions. Thus, some facile, simple and general methods were developed to construct drug/prodrug-based amorphous NCPs for therapy. In 2008, Lin and coworkers first reported a NCPs forming from Tb^{3+} and platinum prodrug by poor solvent precipitation method for drug delivery.[128] As shown in Fig. 14, NCP-1 was built from cisplatin-based prodrug with two carboxyl groups and lanthanide metal ions (Tb^{3+}), then NCP-1′ obtained by coating a silica shell on

NCP-1 to improve the water stability (NCP-1′-a with a silica shell thickness of ~ 2 nm, NCP-1′-b with ~ 7 nm silica shell). Furthermore, a targeted peptide c(RGDfK) was modified on silica shell *via* covalent conjugation. They demonstrated that the thickness of the silica shell could improve the stability, and also efficiently control the release of Pt species for targeted drug delivery.

In their follow up work, Lin and his team refined the synthetic strategy and formulated a series of NCPs for anti-cancer therapy. As shown in Fig. 15, drugs with double carboxyl
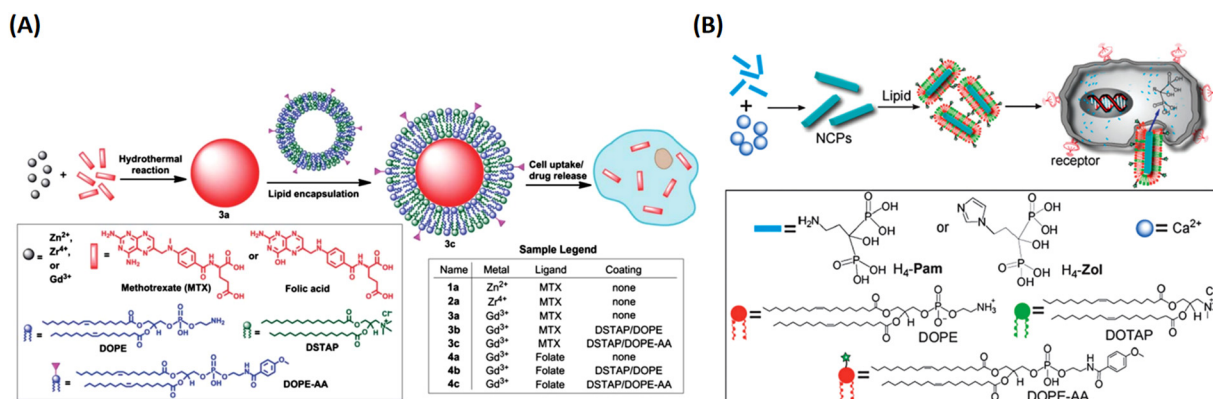

Fig. 15 The synthesis of NCPs *via* hydrothermal reaction and functionalization with a lipid bilayer for targeted delivery and controlled release. (A) MTX-based NCPs for targeted delivery to cancer cells;[129] Copyright 2012, *Chemical science*. (B) H_4-Pam/H_4-Zol-based NCPs and their targeted delivery to cancer cells.[130] Copyright 2012, *Chemical Communications* (Camb).

3284 | *J. Mater. Chem. B*, 2023, **11**, 3273–3294

This journal is © The Royal Society of Chemistry 2023

Fig. 16 The construction of lipid-coated NCPs *via* reverse microemulsion for delivery. (A) General procedure for self-assembly of NCPs with lipid and PEG coatings; (B) schematic showing endocytosis of NCPs and subsequent reduction of prodrug ligands by intracellular reducing agents, such as glutathione, to release cytotoxic cisplatin and oxaliplatin.[132] Copyright 2014, *Nature Communications*.

(methotrexate, folic acid) or bisphosphonates (pamidronate, zoledronate) as building blocks coordinate with metal connecting (Zn^{2+}, Zr^{4+}, Gd^{3+}, Ca^{2+}) to form different morphology NCPs by hydrothermal reaction. Encapsulation of the NCPs within a functionalized lipid bilayer could achieve targeted delivery and controlled release to cancer cells.[129–131] Subsequently, they further developed reverse microemulsion and pegylated method to obtain multifunctional NCPs for *in vivo* therapy. They constructed lipid-coated NCPs *via* reverse microemulsion, and then modified PEG-functionalized lipid or even siRNA-functionalized lipid (Fig. 16). The as-prepared NCPs exhibited excellent blood circulation, superior potency and efficacy for chemotherapy, gene silencing, immunotherapy or their combined therapy.[132–140] Importantly, they have made significant progress and promoted clinical translation of some NCPs.

Inspired by these, Liu's group fabricated nanoscale metal–organic particles (NMOPs) composed of Mn^{2+} ions and a NIR dye, IR825 photothermal agents *via* coordinated self-assembly,

obtaining Mn-IR825 NMOPS as the core. Then, a shell of polydopamine (PDA) was also coated along with PEG functionalization, achieving Mn-IR825@PDA-PEG NMOPs.[141] Among them, IR825 exhibited strong photothermal conversion and high photostability for efficient photothermal therapy (PTT), and Mn^{2+} ions were endowed with T1-weighted MR imaging. Thus, Mn-IR825@PDA-PEG NMOPs can be applied for MRI-guided PTT. Furthermore, the Mn-IR825 core was mixed with Hf^{4+} ions *via* post-synthesis cation exchange, and then they obtained co-doped Mn/Hf-IR825@PDA-PEG NMOPs. Due to Hf^{4+} with its excellent computed tomography (CT) enhancement ability and radio-sensitization (RT) capability, Mn/Hf-IR825@PDA-PEG NMOPs can be utilized for MR&CT&PA multi-mode imaging and PTT&RT synergistic treatment of tumors with high therapeutic efficacy.[137]

Recently, we designed and constructed novel NCPs, integrating two prodrugs (Pt(IV) prodrug and NO donor) as organic ligands and Fe^{3+} as coordinative centers.[142] As shown in Fig. 17,

Fig. 17 The construction of integrated bio-orthogonal NCPs and their therapeutic mechanism of tumor-specific initiating cascade reactions.[142] Copyright 2022, *JACS* Au.
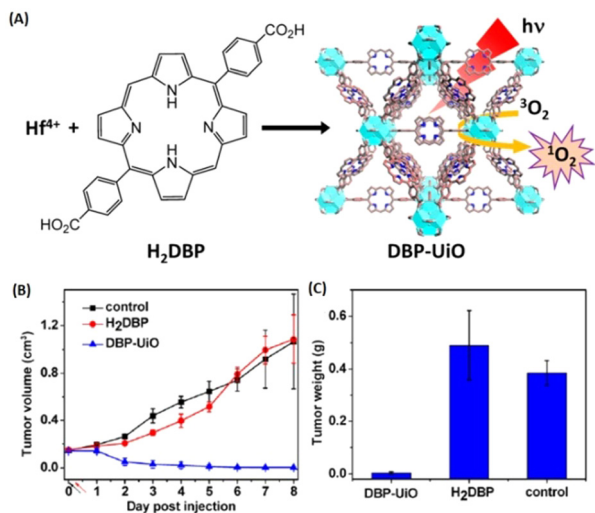
Fig. 18 MOFs constructing with porphyrin derivative-based linkers for highly efficient PDT. (A) Synthesis of Hf-DBP NMOF and the schematic description of the $^1O_2$ generation process. (B) Tumor growth inhibition curve after PDT treatment. Black and red arrows refer to injection and irradiation time points, respectively. (C) Tumor weight after PDT treatment.[143] Copyright 2014, *Journal of the American Chemical Society*.

this unique NCPs contained two prodrugs of bio-orthogonal chemistry, the masked trigger of the Pt(IV) prodrug and the caged active group of the NO donor. In a tumor microenvironment, the Pt(IV) prodrug can be reduced to catalytically active Pt(II) cisplatin, which triggers depropargylation of the NO donor to release high levels of NO. Thus, the DNA crosslinking effect of Pt(II) cisplatin and the anticancer activity of NO achieved synergistic therapy for triple-negative breast cancer.

Compared to the above-mentioned small molecular therapeutic agents as building blocks, porphyrins and porphyrin derivatives are macromolecular heterocyclic compounds with molecular rigidity, which have been widely used as photosensitizers (PSs) for photodynamic therapy (PDT). Therefore, the development of porphyrinic MOFs for PDT has attracted

tremendous attention. For instance, Lin and coworkers were the first to construct MOFs with porphyrin derivative-based linkers for highly effective PDT.[143] As shown in Fig. 18, the porphyrinic MOFs (DBP-UiO) were built from a porphyrin derivative, 5,15-di(p-benzoato)porphyrin (H$_2$DBP) linkers and Hf$_{12}$(μ_3-O)$_8$(μ_3-OH)$_8$(μ_2-OH)$_6$ by a solvothermal reaction. The as-prepared DBP-UiO MOFs were highly stable in physiological media, and efficiently generated singlet oxygen ($^1O_2$) upon 640 nm irradiation. They demonstrated high anticancer efficacy of DBP-UiO-enabled PDT *in vitro* cytotoxicity and human head and neck cancer models *in vivo*. Furthermore, they optimized the design of the chlorin-based MOFs by reducing the ligands of 5,15-di(p-benzoato)chlorin (H$_2$DBC) in DBC-UiO.[144] Compared with DBP-UiO, DBC-UiO was redshifted by 13 nm to provide improved tissue penetration, and the extinction coefficient at the lowest energy Q-band was increased 11-fold to generate more efficient $^1O_2$ for PDT. The combination of Hf-porphyrin or Hf-porphyrinic derivate MOF-mediated PDT with immunotherapy has been explored.[145,146]

Subsequently, several other research groups have developed more porphyrinic MOFs (PCN-224, PCN-222, MOF-545 *etc.*) for PDT or PDT-based combination therapy.[147–162] For example, Zhou and colleagues reported a size-controlled synthesis of Zr-TCPP MOF (named PCN-224) ranging from 30 nm to 190 nm and functionalized with folic acid (FA) onto Zr$_6$ cluster in PCN-224 for targeted PDT.[148] They demonstrated that PCN-224 of 90 nm has preferential cellular uptake and remarkable PDT efficacy over other sizes. By using PCN-224, Zhang and coworkers constructed a cancer cell membrane-camouflaged cascade bioreactor by loading glucose oxidase (GOx) and catalase on the surface of PNC-224 for targeted starvation therapy-PDT synergistic antitumor therapy.[149]

Noteworthily, the controlled generation of ROS in PDT has attracted considerable attention. Zhou and coworkers developed photochromic porphyrin-based MOFs for reversible control of $^1O_2$ generation.[147] As shown in Fig. 19, using 1,2-bis (2-methyl-5-(pyridin-4-yl)thiophen-3-yl)cyclopent-1-ene (BPDTE)
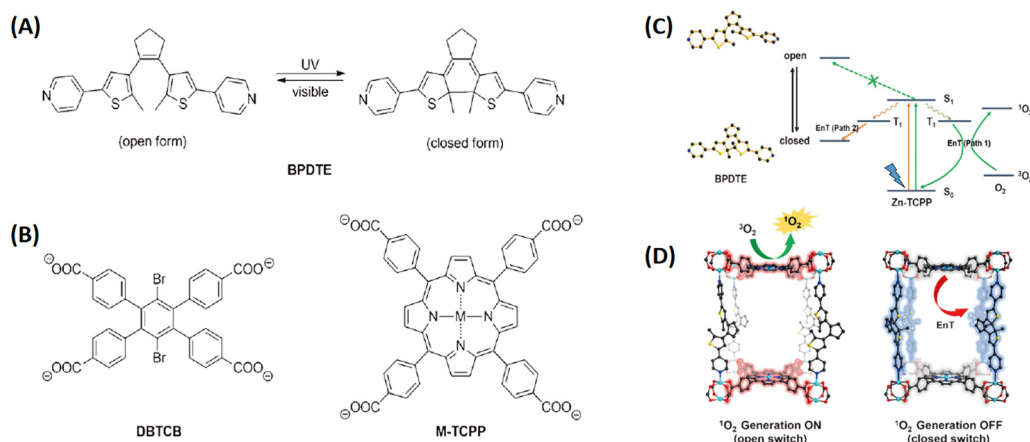

Fig. 19 Photochromic porphyrin-based MOFs used to reversibly control $^1O_2$ generation. (A) Photoisomerization of BPDTE under UV and visible light. (B) Structures of ligands consist of two-dimensional layers in PC–PCN and SO–PCN, respectively. (C) Proposed mechanism of energy transfer (EnT) in SO–PCN. (D) Illustration of switching operation in SO–PCN.[147] Copyright 2015, *Angew. Chem.-Int. Edit.*

3286 | *J. Mater. Chem. B*, 2023, **11**, 3273–3294

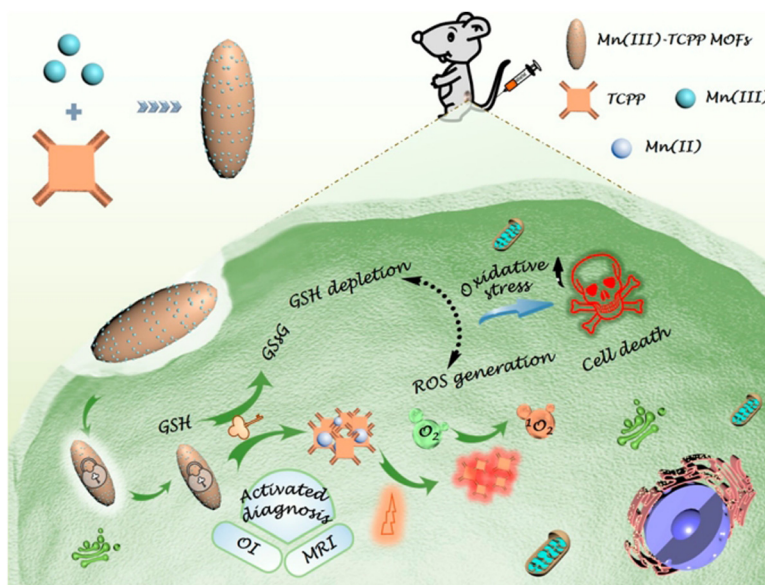This journal is © The Royal Society of Chemistry 2023

Fig. 20 Schematic illustration of an endocytosis Mn(III)-TCPP MOF nanosystem for MRI- and OI-guided PDT by controlled ROS generation and GSH depletion after being unlocked by overexpressed GSH in tumor cells.[159] Copyright 2019, *ACS Nano*.

as a photochromic switch, they designed two MOFs by solvothermal reaction of BPDTE, TCPP or tetratopic carboxylate linker DBTCB and Zn^{2+} to obtained SO-PCN and PC-PCN. Meanwhile, SO-PCN has been demonstrated to regulate $^1O_2$ generation under UV/visible irradiation. Recently, Zhang *et al.* utilized Mn(III) as a sealer to quench the fluorescence of TCPP and inhibit ROS generation, designing an ''inert'' Mn(III)-TCPP MOFs.[159] The as-prepared MOFs could be activated by the overexpression of GSH in tumor cells, and consumed GSH to release Mn(II) ions and free TCPP. So, the unlocking MOFs exhibited Mn(II)-based MRI and TCPP-based OI. On the other hand, the consumption of GSH could effectively control ROS production and enhance the efficacy of TCPP-based PDT (Fig. 20).

3.2. Active metals

Some active metal centers have also been explored for therapy in recent years, such as Ag^+, Cu^+, Co^{2+}, and Zn^{2+} ions are known for their antibacterial activities. Therefore, these active metal ions in MOFs/NCPs exhibited corresponding therapeutic effects.

Due to the excellent antibacterial activity of Ag^+ ions, Ag-based MOFs/NCPs have been synthesized to deliver Ag^+ ions for antibacterial therapy. Fromm and coworkers formulated a nanostructured silver coordination polymer compounds, and deposited the as-prepared compounds onto the surface of a gold–titanium alloy as an antimicrobial agent for dental implant and restorative materials.[163] They further demonstrated the biochemical and molecular mechanisms of the bactericidal activity of Ag^+ ions, which could be attributed to the ability of Ag^+ ions to inactivate enzymes by binding thiol groups in amino acids, and promote iron release with $^\bullet OH$ production and subsequent DNA damage.[164] Jaffrès *et al.*

synthesized Ag_3(3-phosphonobenzoate) MOF for the sustainable release of Ag^+ with high bactericidal activity against 6 bacterial strains.[165] Afterwards, several new silver MOFs were constructed for antimicrobial therapy.[166,167]

Recently, transition metal ions (Cu^+, Co^{2+}, Fe^{3+}, *etc.*) as metal centers in coordination polymers (CPs) presented good bactericidal action and anticancer activities.[168] The Zamaro group synthesized a Cu-based MOF, named HKUST-1, and successfully applied HKUST-1 to inhibit the growth of *S. cerevisiae* and *G. candidum* because of the release of Cu^+ ions during the progressive degradation.[169] Liu *et al.* designed a novel Co-based MOF (Co-TDM) with high bactericidal activity, which was constructed from Co^{2+} ions and octa-topic carboxylate ligand, tetrakis [[(3,5-dicarboxyphenyl)-oxamethyl] methane (TDM^{8-}).[170] As shown in Fig. 21, the mechanism of the bactericidal activities could be observed in six steps: (1) diffusion-directed lipid-oxidation, (2) direct interaction, (3) reaction-oxygen species generation, (4) cation transport interruption, (5) chelation effects, and (6) membrane depolarization. Co^{2+} ions served as active sites to catalyze lipid peroxidation. Thus, the bacterial membrane ruptured and the bacteria were inactivated. A few Co-based MOFs also have been developed to combat bacteria.[171,172]

High atomic (Z) number elements, such as Au and HfO_2, with high X-ray absorption coefficients, have been deemed as promising radioenhancers for anticancer therapy. Inspired by this, Lin and coworkers synthesized Hf-based MOFs as highly effective radioenhancers for radiotherapy (RT). Importantly, when combined with the anti-programmed death-ligand 1 (anti-PD-L1) antibody, the Hf-based MOF-mediated low-dose RT with immunotherapy achieved local therapeutic effects of RT and distant tumor therapy *via* immunity.[173] As shown in Fig. 22, Hf_{12}-DBA could efficiently generate $^\bullet OH$ upon X-ray

This journal is © The Royal Society of Chemistry 2023

J. Mater. Chem. B, 2023, **11**, 3273–3294 | **3287**

Fig. 21 The mechanism of bactericidal activities using Co-TDM single crystals as disinfectants: six steps synergistically contribute to the bactericidal efficacy.[170] Copyright 2012, *Advanced Healthcare Materials*.

irradiation to enhance RT for local tumor therapy. The immunogenic cell death of RT led to tumor antigen release, and when used in combination with the anti-PD-L1 antibody, caused regression in distant tumors *via* systemic antitumor immunity.

3.3. The combination of active metals and ligands

Nowadays, combination/synergistic therapy is widely used to boost the therapeutic effect. In this regard, MOFs combining bioactive cations with therapeutic ligands could achieve a highly effective synergistic treatment.

Spencer *et al.* synthesized a series of bismuth-dicarboxylate-deferiprone coordination networks, wherein both the ligand (deferiprone) and metal center (Bi^{3+} ions) in the coordination networks played their therapy roles for the inhibition of *H. pylori* growth.[174] Blanco-Prieto and colleagues constructed a novel BioMIL-5 based on Zn^{2+} ions and azelaic acid *via* hydrothermal method, and both components of BioMIL-5 exhibited high antibacterial activity and interesting dermatological property.[175] The progressive simultaneous release of active Zn^{2+} and azelaic acid from BioMIL-5, in both water and culture

Fig. 22 Hf-based MOFs served as highly efficient radiation enhancers for radiotherapy (RT). (A) Illustration of efficient hydroxyl radical generation upon X-ray irradiation and diffusion through porous Hf_{12}-DBA nanoplates; (B) Abscopal effect of nMOF-mediated RT and immune checkpoint blockade using fractionated X-rays.[173] Copyright 2018, *Nature Communications*.

3288 | *J. Mater. Chem. B*, 2023, **11**, 3273–3294

This journal is © The Royal Society of Chemistry 2023

Fig. 23 NO donor-constructed Fe-based NCPs for NO-CDT synergistic antitumor therapy. (A) Schematic illustration of Fe(III)-BNCP and Fe(II)-BNCP preparation; (B) NO-CDT synergistic therapy of Fe(II)-BNCP in tumor cells.[176] Copyright 2019, *Nano Letters*.

media, not only have continuous antibacterial properties for as long as 7 days to inhibit the growth of Gram-positive *S. epidermidis*, but also provide complementary beneficials for skin disorders treatment.

Besides the combined antimicrobial therapy, the synergistic and combined therapy of cancer has also been developed using MOFs/NCPs built up from active metal and therapeutic ligands. For example, we constructed NCPs based on NO donor and iron ions for synergistic NO and chemodynamic therapy (CDT) of liver cancer.[176] As shown in Fig. 23, a GSH-sensitive NO donor with two carboxyl groups coordinated with iron ions to form

NCP *via* simple precipitation and partial ion exchange. The NO donors in Fe(II)-BNCP released NO and the Fe^{2+} ions exerted Fenton activity to generate ROS in tumor microenvironments triggered by GSH and induced by H_2O_2, respectively. In addition, the synergistic NO-CDT effect of Fe(II)-BNCP has been applied to retard the tumor growth in Heps xenograft ICR mouse models. Liu *et al.* synthesized a carrier-free MOFs system based on Hf^{4+} and TCPP that was used for TCPP-mediated PDT and Hf^{4+}-enabled radiotherapy (RT).[177] Lin and colleagues engineered a Cu-porphyrin MOF for synergistic hormone-triggered CDT and light-triggered PDT.[178] As shown in Fig. 24, pH-triggered MOF decomposed to release Cu^{2+} ions and porphyrins for estradiol-induced CDT and light-driven PDT, respectively. Furthermore, with the combination of MOF-mediated CDT/PDT with anti-PD-L1 immunotherapy, the local and distant tumors effectively regressed. In addition, the combination of porphyrinic MOF-based PDT and active metal ions for synergistic therapy have been described in the part of porphyrinic MOFs.

4. Conclusion and outlooks

We have summarized the main applications of nanoscale MOFs or NCPs in the field of therapy, which has achieved growing development. In the early state, MOF-based porous materials were extensively used as carriers to deliver a variety of drugs, including small molecule chemical drugs, proteins, nucleic acids, saccharides, antigens, adjuvants, and gasotransmitters. Compared with other nanocarriers, MOF-based delivery systems have shown some intrinsic advantages of biodegradability, high porosity, adjustability of components, the flexibility of modification and controlled release. Although MOF-based nanocarriers have made enormous progress in the field of drug delivery, their therapeutic applications are still in their infancy.

Fig. 24 Synergy of checkpoint blockade immunotherapy and MOF-mediated CDT/PDT triggered by both hormone and light stimulation.[178] Copyright 2019, *Chemistry*.

This journal is © The Royal Society of Chemistry 2023

J. Mater. Chem. B, 2023, **11**, 3273–3294 | **3289**

MOFs or NCPs were then derived from therapeutic ligands, active metal ions or their combination, developing as therapeutic agents, which greatly facilitated the therapy of various diseases.

In recent years, MOFs have achieved tremendous advances and indicated great prospects in the field of biomedicine. However, there still remain critical challenges: (1) the biological safety of MOFs is worrying. (2) The stability of MOFs in biological systems is not satisfactory. (3) The synthesis conditions are not friendly. (4) The metabolic pathway is ambiguous. (5) The structure and druggability of MOFs need to be improved. (6) The strategies for large-scale fabrication of MOFs are rare. (7) Most targeting modification approaches are tedious and complicated. These existing problems greatly hinder the clinical transformation of MOFs.

Taken together, the challenges of MOFs need to be overcome urgently before realizing their clinical applications. We still have much to do to achieve the safe and efficient application of MOF-based therapy. To achieve this, we call for more researchers to devote attention toward advancing and translating MOF-based nanodrugs into clinic. We also hope this review will help readers understand the current development of MOF-based therapy, including their advantages and challenges, and will drive chemists, materials scientists, biologists, pharmacists and clinicians to participate in this research and to benefit patients for achieving clinical application of MOF-based therapy as soon as possible.

Conflicts of interest

There are no conflicts to declare.

Acknowledgements

References

1 K. Zhang, A. G. Mikos, R. L. Reis and X. Zhang, *Bioact. Mater.*, 2022, **18**, 337–338.

2 D. H. Kohn, *Matter*, 2019, **1**, 1114–1115.

3 X. Guo, H. Xu, W. Li, Y. Liu, Y. Shi, Q. Li and H. Pang, *Adv. Sci.*, 2023, **10**, e2206084.

4 T. Chen, F. Wang, S. Cao, Y. Bai, S. Zheng, W. Li, S. Zhang, S. X. Hu and H. Pang, *Adv. Mater.*, 2022, **34**, e2201779.

5 P. Geng, L. Wang, M. Du, Y. Bai, W. Li, Y. Liu, S. Chen, P. Braunstein, Q. Xu and H. Pang, *Adv. Mater.*, 2022, **34**, e2107836.

6 X. Joseph, V. Akhil, A. Arathi and P. V. Mohanan, *Mater. Sci. Eng., B*, 2022, **279**, 115680–115695.

7 Y. Li, *Curr. Org. Chem.*, 2016, **20**, 1754–1755.

8 T. V. Safronova, *Inorg. Mater.*, 2021, **57**, 443–474.

9 P. Horcajada, C. Serre, M. Vallet-Regi, M. Sebban, F. Taulelle and G. Ferey, *Angew. Chem., Int. Ed.*, 2006, **45**, 5974–5978.

10 P. Horcajada, C. Serre, G. Maurin, N. A. Ramsahye, F. Balas, M. Vallet-Regi, M. Sebban, F. Taulelle and G. Ferey, *J. Am. Chem. Soc.*, 2008, **130**, 6774–6780.

11 J. An, S. J. Geib and N. L. Rosi, *J. Am. Chem. Soc.*, 2009, **131**, 8376–8377.

12 P. Horcajada, T. Chalati, C. Serre, B. Gillet, C. Sebrie, T. Baati, J. F. Eubank, D. Heurtaux, P. Clayette, C. Kreuz, J. S. Chang, Y. K. Hwang, V. Marsaud, P. N. Bories, L. Cynober, S. Gil, G. Ferey, P. Couvreur and R. Gref, *Nat. Mater.*, 2010, **9**, 172–178.

13 T. Chalati, P. Horcajada, P. Couvreur, C. Serre, M. Ben Yahia, G. Maurin and R. Gref, *Nanomedicine*, 2011, **6**, 1683–1695.

14 V. Agostoni, T. Chalati, P. Horcajada, H. Willaime, R. Anand, N. Semiramoth, T. Baati, S. Hall, G. Maurin, H. Chacun, K. Bouchemal, C. Martineau, F. Taulelle, P. Couvreur, C. Rogez-Kreuz, P. Clayette, S. Monti, C. Serre and R. Gref, *Adv. Healthcare Mater.*, 2013, **2**, 1630–1637.

15 S. Rojas, E. Quartapelle-Procopio, F. J. Carmona, M. A. Romero, J. A. R. Navarro and E. Barea, *J. Mater. Chem. B*, 2014, **2**, 2473–2477.

16 E. Bellido, T. Hidalgo, M. V. Lozano, M. Guillevic, R. Simón-Vázquez, M. J. Santander-Ortega, Á. González-Fernández, C. Serre, M. J. Alonso and P. Horcajada, *Adv. Healthcare Mater.*, 2015, **4**, 1246–1257.

17 V. Rodriguez-Ruiz, A. Maksimenko, R. Anand, S. Monti, V. Agostoni, P. Couvreur, M. Lampropoulou, K. Yannakopoulou and R. Gref, *J. Drug Targeting*, 2015, **23**, 759–767.

18 M. Al Haydar, H. R. Abid, B. Sunderland and S. Wang, *Drug Des., Dev. Ther.*, 2017, **11**, 2685–2695.

19 T. Simon-Yarza, M. Gimenez-Marques, R. Mrimi, A. Mielcarek, R. Gref, P. Horcajada, C. Serre and P. Couvreur, *Angew. Chem., Int. Ed.*, 2017, **56**, 15565–15569.

20 A. Golmohamadpour, B. Bahramian, M. Khoobi, M. Pourhajibagher, H. R. Barikani and A. Bahador, *Photodiagn. Photodyn. Ther.*, 2018, **23**, 331–338.

21 I. Ghaffar, M. Imran, S. Perveen, T. Kanwal, S. Saifullah, M. F. Bertino, C. J. Ehrhardt, V. K. Yadavalli and M. R. Shah, *Mater. Sci. Eng., C*, 2019, **105**, 110111–110120.

22 D. Cunha, C. Gaudin, I. Colinet, P. Horcajada, G. Maurin and C. Serre, *J. Mater. Chem. B*, 2013, **1**, 1101–1108.

23 C. He, K. Lu, D. Liu and W. Lin, *J. Am. Chem. Soc.*, 2014, **136**, 5181–5184.

24 X. Zhu, J. Gu, Y. Wang, B. Li, Y. Li, W. Zhao and J. Shi, *Chem. Commun.*, 2014, **50**, 8779–8782.

25 L. L. Tan, H. Li, Y. Zhou, Y. Zhang, X. Feng, B. Wang and Y. W. Yang, *Small*, 2015, **11**, 3807–3813.

26 M. Filippousi, S. Turner, K. Leus, P. I. Siafaka, E. D. Tseligka, M. Vandichel, S. G. Nanaki, I. S. Vizirianakis, D. N. Bikiaris, P. Van der Voort and G. Van Tendeloo, *Int. J. Pharm.*, 2016, **509**, 208–218.

27 I. A. Lazaro, S. Haddad, S. Sacca, C. Orellana-Tavra, D. Fairen-Jimenez and R. S. Forgan, *Chem*, 2017, **2**, 561–578.

3290 | *J. Mater. Chem. B*, 2023, **11**, 3273–3294

This journal is © The Royal Society of Chemistry 2023

28 I. A. Lazaro, S. Haddad, J. M. Rodrigo-Munoz, C. Orellana-Tavra, V. del Pozo, D. Fairen-Jimenez and R. S. Forgan, *ACS Appl. Mater. Interfaces*, 2018, **10**, 5255–5268.

29 F. Ke, Y.-P. Yuan, L.-G. Qiu, Y.-H. Shen, A.-J. Xie, J.-F. Zhu, X.-Y. Tian and L.-D. Zhang, *J. Mater. Chem.*, 2011, **21**, 3843–3848.

30 K. Lu, T. Aung, N. Guo, R. Weichselbaum and W. Lin, *Adv. Mater.*, 2018, **30**, e1707634.

31 Y. A. Li, X. D. Zhao, H. P. Yin, G. J. Chen, S. Yang and Y. B. Dong, *Chem. Commun.*, 2016, **52**, 14113–14116.

32 C. Y. Sun, C. Qin, X. L. Wang, G. S. Yang, K. Z. Shao, Y. Q. Lan, Z. M. Su, P. Huang, C. G. Wang and E. B. Wang, *Dalton Trans.*, 2012, **41**, 6906–6909.

33 L. He, T. Wang, J. An, X. Li, L. Zhang, L. Li, G. Li, X. Wu, Z. Su and C. Wang, *CrystEngComm*, 2014, **16**, 3259–3263.

34 J. Zhuang, C. H. Kuo, L. Y. Chou, D. Y. Liu, E. Weerapana and C. K. Tsung, *ACS Nano*, 2014, **8**, 2812–2819.

35 C. Adhikari, A. Das and A. Chakraborty, *Mol. Pharmaceutics*, 2015, **12**, 3158–3166.

36 M. R. di Nunzio, V. Agostoni, B. Cohen, R. Gref and A. Douhal, *J. Med. Chem.*, 2014, **57**, 411–420.

37 S. Nagata, K. Kokado and K. Sada, *Chem. Commun.*, 2015, **51**, 8614–8617.

38 L.-L. Tan, N. Song, S. X.-A. Zhang, H. Li, B. Wang and Y.-W. Yang, *J. Mater. Chem. B*, 2016, **4**, 135–140.

39 X. G. Wang, Z. Y. Dong, H. Cheng, S. S. Wan, W. H. Chen, M. Z. Zou, J. W. Huo, H. X. Deng and X. Z. Zhang, *Nanoscale*, 2015, **7**, 16061–16070.

40 H. Zhang, Q. Li, R. Liu, X. Zhang, Z. Li and Y. Luan, *Adv. Funct. Mater.*, 2018, **28**, 1802830–1802839.

41 B. P. Mugaka, S. Zhang, R.-Q. Li, Y. Ma, B. Wang, J. Hong, Y.-H. Hu, Y. Ding and X.-H. Xia, *ACS Appl. Mater. Interfaces*, 2021, **13**, 11195–11204.

42 K. M. Taylor-Pashow, J. Della Rocca, Z. Xie, S. Tran and W. Lin, *J. Am. Chem. Soc.*, 2009, **131**, 14261–14263.

43 S. Javanbakht, A. Hemmati, H. Namazi and A. Heydari, *Int. J. Biol. Macromol.*, 2019, **155**, 876–882.

44 Y. Li, X. Li, Q. Guan, C. Zhang, T. Xu, Y. Dong, X. Bai and W. Zhang, *Int. J. Nanomed.*, 2017, **12**, 1465–1474.

45 S. Li, K. Wang, Y. Shi, Y. Cui, B. Chen, B. He, W. Dai, H. Zhang, X. Wang, C. Zhong, H. Wu, Q. Yang and Q. Zhang, *Adv. Funct. Mater.*, 2016, **26**, 2715–2727.

46 I. B. Vasconcelos, T. G. d Silva, G. C. G. Militão, T. A. Soares, N. M. Rodrigues, M. O. Rodrigues, N. B. d Costa, R. O. Freire and S. A. Junior, *RSC Adv.*, 2012, **2**, 9437–9442.

47 H. Zheng, Y. Zhang, L. Liu, W. Wan, P. Guo, A. M. Nystrom and X. Zou, *J. Am. Chem. Soc.*, 2016, **138**, 962–968.

48 M. Zheng, S. Liu, X. Guan and Z. Xie, *ACS Appl. Mater. Interfaces*, 2015, 7, 22181–22187.

49 A. Tiwari, A. Singh, N. Garg and J. K. Randhawa, *Sci. Rep.*, 2017, **7**, 1–12.

50 H. Zhang, W. Jiang, R. Liu, J. Zhang, D. Zhang, Z. Li and Y. Luan, *ACS Appl. Mater. Interfaces*, 2017, **9**, 19687–19697.

51 X. Chen, R. Tong, Z. Shi, B. Yang, H. Liu, S. Ding, X. Wang, Q. Lei, J. Wu and W. Fang, *ACS Appl. Mater. Interfaces*, 2018, **10**, 2328–2337.

52 Z. Shi, X. Chen, L. Zhang, S. Ding, X. Wang, Q. Lei and W. Fang, *Biomater. Sci.*, 2018, **6**, 2582–2590.

53 X. Zhang, L. Liu, L. Huang, W. Zhang, R. Wang, T. Yue, J. Sun, G. Li and J. Wang, *Nanoscale*, 2019, **11**, 9468–9477.

54 F.-M. Zhang, H. Dong, X. Zhang, X.-J. Sun, M. Liu, D.-D. Yang, X. Liu and J.-Z. Wei, *ACS Appl. Mater. Interfaces*, 2017, **9**, 27332–27337.

55 K. Xing, R. Fan, F. Wang, H. Nie, X. Du, S. Gai, P. Wang and Y. Yang, *ACS Appl. Mater. Interfaces*, 2018, **10**, 22746–22756.

56 P. P. Bag, D. Wang, Z. Chen and R. Cao, *Chem. Commun.*, 2016, **52**, 3669–3672.

57 F. R. Lucena, L. C. de Araujo, D. Rodrigues Mdo, T. G. da Silva, V. R. Pereira, G. C. Militao, D. A. Fontes, P. J. Rolim-Neto, F. F. da Silva and S. C. Nascimento, *Biomed. Pharmacother.*, 2013, **67**, 707–713.

58 L. Q. Wei, Q. Chen, L. L. Tang, C. Zhuang, W. R. Zhu and N. Lin, *Dalton Trans.*, 2016, **45**, 3694–3697.

59 Z. Wu, N. Hao, H. Zhang, Z. Guo, R. Liu, B. He and S. Li, *Biomater. Sci.*, 2017, **5**, 1032–1040.

60 Q. Hu, J. Yu, M. Liu, A. Liu, Z. Dou and Y. Yang, *J. Med. Chem.*, 2014, **57**, 5679–5685.

61 T. Kundu, S. Mitra, P. Patra, A. Goswami, D. D. Diaz and R. Banerjee, *Chem. – Eur. J.*, 2014, **20**, 10514–10518.

62 K. Jiang, L. Zhang, Q. Hu, D. Zhao, T. Xia, W. Lin, Y. Yang, Y. Cui, Y. Yang and G. Qian, *J. Mater. Chem. B*, 2016, **4**, 6398–6401.

63 W. Lin, Q. Hu, J. Yu, K. Jiang, Y. Yang, S. Xiang, Y. Cui, Y. Yang, Z. Wang and G. Qian, *ChemPlusChem*, 2016, **81**, 804–810.

64 Y. Yang, Q. Hu, Q. Zhang, K. Jiang, W. Lin, Y. Yang, Y. Cui and G. Qian, *Mol. Pharmaceutics*, 2016, **13**, 2782–2786.

65 M. H. Teplensky, M. Fantham, P. Li, T. C. Wang, J. P. Mehta, L. J. Young, P. Z. Moghadam, J. T. Hupp, O. K. Farha, C. F. Kaminski and D. Fairen-Jimenez, *J. Am. Chem. Soc.*, 2017, **139**, 7522–7532.

66 G. N. Lucena, R. C. Alves, M. P. Abucafy, L. A. Chiavacci, I. C. da Silva, F. R. Pavan and R. C. Galvao Frem, *J. Solid State Chem.*, 2018, **260**, 67–72.

67 L. L. Tan, H. Li, Y. C. Qiu, D. X. Chen, X. Wang, R. Y. Pan, Y. Wang, S. X. Zhang, B. Wang and Y. W. Yang, *Chem. Sci.*, 2015, **6**, 1640–1644.

68 M. Kotzabasaki, I. Galdadas, E. Tylianakis, E. Klontzas, Z. Cournia and G. E. Froudakis, *J. Mater. Chem. B*, 2017, **5**, 3277–3282.

69 B. Yang, M. Shen, J. Liu and F. Ren, *Pharm. Res.*, 2017, **34**, 2440–2450.

70 G. Tan, Y. Zhong, L. Yang, Y. Jiang, J. Liu and F. Ren, *Chem. Eng. J.*, 2020, **390**, 124446–124458.

71 X. Du, R. Fan, L. Qiang, K. Xing, H. Ye, X. Ran, Y. Song, P. Wang and Y. Yang, *ACS Appl. Mater. Interfaces*, 2017, **9**, 28939–28948.

72 B. Liu, H. Li, X. Xu, X. Li, N. Lv, V. Singh, J. F. Stoddart, P. York, X. Xu, R. Gref and J. Zhang, *Int. J. Pharm.*, 2016, **514**, 212–219.

73 K. J. Hartlieb, D. P. Ferris, J. M. Holcroft, I. Kandela, C. L. Stern, M. S. Nassar, Y. Y. Botros and J. F. Stoddart, *Mol. Pharmaceutics*, 2017, **14**, 1831–1839.

This journal is © The Royal Society of Chemistry 2023

J. Mater. Chem. B, 2023, **11**, 3273–3294 | **3291**

74 H. Li, N. Lv, X. Li, B. Liu, J. Feng, X. Ren, T. Guo, D. Chen, J. Fraser Stoddart, R. Gref and J. Zhang, *Nanoscale*, 2017, **9**, 7454–7463.

75 J.-Q. Sha, X.-H. Zhong, L.-H. Wu, G.-D. Liu and N. Sheng, *RSC Adv.*, 2016, **6**, 82977–82983.

76 T. J. Pisklak, M. Macías, D. H. Coutinho, R. S. Huang and K. J. Balkus, *Top. Catal.*, 2006, **38**, 269–278.

77 V. Lykourinou, Y. Chen, X. S. Wang, L. Meng, T. Hoang, L. J. Ming, R. L. Musselman and S. Ma, *J. Am. Chem. Soc.*, 2011, **133**, 10382–10385.

78 F. Lyu, Y. Zhang, R. N. Zare, J. Ge and Z. Liu, *Nano Lett.*, 2014, **14**, 5761–5765.

79 K. Liang, R. Ricco, C. M. Doherty, M. J. Styles, S. Bell, N. Kirby, S. Mudie, D. Haylock, A. J. Hill, C. J. Doonan and P. Falcaro, *Nat. Commun.*, 2015, **6**, 7240–7247.

80 F. K. Shieh, S. C. Wang, C. I. Yen, C. C. Wu, S. Dutta, L. Y. Chou, J. V. Morabito, P. Hu, M. H. Hsu, K. C. Wu and C. K. Tsung, *J. Am. Chem. Soc.*, 2015, **137**, 4276–4279.

81 X. Wu, J. Ge, C. Yang, M. Hou and Z. Liu, *Chem. Commun.*, 2015, **51**, 13408–13411.

82 J. Cui, Y. Feng, T. Lin, Z. Tan, C. Zhong and S. Jia, *ACS Appl. Mater. Interfaces*, 2017, **9**, 10587–10594.

83 S. Y. Li, H. Cheng, B. R. Xie, W. X. Qiu, J. Y. Zeng, C. X. Li, S. S. Wan, L. Zhang, W. L. Liu and X. Z. Zhang, *ACS Nano*, 2017, **11**, 7006–7018.

84 T.-T. Chen, J.-T. Yi, Y.-Y. Zhao and X. Chu, *J. Am. Chem. Soc.*, 2018, **140**, 9912–9920.

85 G. Cheng, W. Li, L. Ha, X. Han, S. Hao, Y. Wan, Z. Wang, F. Dong, X. Zou, Y. Mao and S.-Y. Zheng, *J. Am. Chem. Soc.*, 2018, **140**, 7282–7291.

86 L. Zhang, Z. Wang, Y. Zhang, F. Cao, K. Dong, J. Ren and X. Qu, *ACS Nano*, 2018, **12**, 10201–10211.

87 C. Zhang, S. Hong, M. D. Liu, W. Y. Yu, M. K. Zhang, L. Zhang, X. Zeng and X. Z. Zhang, *J. Controlled Release*, 2020, **320**, 159–167.

88 D. Feng, T. F. Liu, J. Su, M. Bosch, Z. Wei, W. Wan, D. Yuan, Y. P. Chen, X. Wang, K. Wang, X. Lian, Z. Y. Gu, J. Park, X. Zou and H. C. Zhou, *Nat. Commun.*, 2015, **6**, 5979–5986.

89 S. Jung, Y. Kim, S. J. Kim, T. H. Kwon, S. Huh and S. Park, *Chem. Commun.*, 2011, **47**, 2904–2906.

90 Y.-H. Shih, S.-H. Lo, N.-S. Yang, B. Singco, Y.-J. Cheng, C.-Y. Wu, I. H. Chang, H.-Y. Huang and C.-H. Lin, *ChemPlusChem*, 2012, **77**, 982–986.

91 W.-L. Liu, S.-H. Lo, B. Singco, C.-C. Yang, H.-Y. Huang and C.-H. Lin, *J. Mater. Chem. B*, 2013, **1**, 928–932.

92 C. Marti-Gastaldo, D. Antypov, J. E. Warren, M. E. Briggs, P. A. Chater, P. V. Wiper, G. J. Miller, Y. Z. Khimyak, G. R. Darling, N. G. Berry and M. J. Rosseinsky, *Nat. Chem.*, 2014, **6**, 343–351.

93 P. A. Sontz, J. B. Bailey, S. Ahn and F. A. Tezcan, *J. Am. Chem. Soc.*, 2015, **137**, 11598–11601.

94 J. B. Bailey, L. Zhang, J. A. Chiong, S. Ahn and F. A. Tezcan, *J. Am. Chem. Soc.*, 2017, **139**, 8160–8166.

95 Y. Chen, S. Han, X. Li, Z. Zhang and S. Ma, *Inorg. Chem.*, 2014, **53**, 10006–10008.

96 Y. Chen, V. Lykourinou, T. Hoang, L.-J. Ming and S. Ma, *Inorg. Chem.*, 2012, **51**, 9156–9158.

97 Y. Chen, V. Lykourinou, C. Vetromile, T. Hoang, L. J. Ming, R. W. Larsen and S. Ma, *J. Am. Chem. Soc.*, 2012, **134**, 13188–13191.

98 X. Lian, A. Erazo-Oliveras, J.-P. Pellois and H.-C. Zhou, *Nat. Commun.*, 2017, **8**, 2075–2084.

99 B. B. Mendes, J. Conniot, A. Avital, D. Yao, X. Jiang, X. Zhou, N. Sharf-Pauker, Y. Xiao, O. Adir, H. Liang, J. Shi, A. Schroeder and J. Conde, *Nat. Rev. Methods Primers*, 2022, **2**, 24–69.

100 R. Nishiyabu, N. Hashimoto, T. Cho, K. Watanabe, T. Yasunaga, A. Endo, K. Kaneko, T. Niidome, M. Murata, C. Adachi, Y. Katayama, M. Hashizume and N. Kimizuka, *J. Am. Chem. Soc.*, 2009, **131**, 2151–2158.

101 M. Zhang, W. Lu, J.-R. Li, M. Bosch, Y.-P. Chen, T.-F. Liu, Y. Liu and H.-C. Zhou, *Inorg. Chem. Front.*, 2014, **1**, 159–162.

102 V. Agostoni, R. Anand, S. Monti, S. Hall, G. Maurin, P. Horcajada, C. Serre, K. Bouchemal and R. Gref, *J. Mater. Chem. B*, 2013, **1**, 4231–4242.

103 Q. Chen, M. Xu, W. Zheng, T. Xu, H. Deng and J. Liu, *ACS Appl. Mater. Interfaces*, 2017, **9**, 6712–6724.

104 W. Morris, W. E. Briley, E. Auyeung, M. D. Cabezas and C. A. Mirkin, *J. Am. Chem. Soc.*, 2014, **136**, 7261–7264.

105 H. Wang, Y. Chen, H. Wang, X. Liu, X. Zhou and F. Wang, *Angew. Chem., Int. Ed.*, 2019, **58**, 7380–7384.

106 S. Peng, B. Bie, Y. Sun, M. Liu, H. Cong, W. Zhou, Y. Xia, H. Tang, H. Deng and X. Zhou, *Nat. Commun.*, 2018, **9**, 1293–1302.

107 Y. Zhang, F. Wang, E. Ju, Z. Liu, Z. Chen, J. Ren and X. Qu, *Adv. Funct. Mater.*, 2016, **26**, 6454–6461.

108 F. Duan, X. Feng, X. Yang, W. Sun, Y. Jin, H. Liu, K. Ge, Z. Li and J. Zhang, *Biomaterials*, 2017, **122**, 23–33.

109 Y. Zhang, C. Liu, F. Wang, Z. Liu, J. Ren and X. Qu, *Chem. Commun.*, 2017, **53**, 1840–1843.

110 W. Ning, Z. Di, Y. Yu, P. Zeng, C. Di, D. Chen, X. Kong, G. Nie, Y. Zhao and L. Li, *Small*, 2018, **14**, e1703812.

111 K. Ni, T. Luo, G. Lan, A. Culbert, Y. Song, T. Wu, X. Jiang and W. Lin, *Angew. Chem., Int. Ed.*, 2020, **59**, 1108–1112.

112 H. Zhang, W. Chen, K. Gong and J. Chen, *ACS Appl. Mater. Interfaces*, 2017, **9**, 31519–31525.

113 B. Xiao, P. S. Wheatley, X. Zhao, A. J. Fletcher, S. Fox, A. G. Rossi, I. L. Megson, S. Bordiga, L. Regli, K. M. Thomas and R. E. Morris, *J. Am. Chem. Soc.*, 2007, **129**, 1203–1209.

114 P. K. Allan, P. S. Wheatley, D. Aldous, M. I. Mohideen, C. Tang, J. A. Hriljac, I. L. Megson, K. W. Chapman, G. De Weireld, S. Vaesen and R. E. Morris, *Dalton Trans.*, 2012, **41**, 4060–4066.

115 A. C. McKinlay, J. F. Eubank, S. Wuttke, B. Xiao, P. S. Wheatley, P. Bazin, J. C. Lavalley, M. Daturi, A. Vimont, G. De Weireld, P. Horcajada, C. Serre and R. E. Morris, *Chem. Mater.*, 2013, **25**, 1592–1599.

116 D. Cattaneo, S. J. Warrender, M. J. Duncan, C. J. Kelsall, M. K. Doherty, P. D. Whitfield, I. L. Megson and R. E. Morris, *RSC Adv.*, 2016, **6**, 14059–14067.

3292 | *J. Mater. Chem. B*, 2023, **11**, 3273–3294

This journal is © The Royal Society of Chemistry 2023

117 S. R. Miller, E. Alvarez, L. Fradcourt, T. Devic, S. Wuttke, P. S. Wheatley, N. Steunou, C. Bonhomme, C. Gervais, D. Laurencin, R. E. Morris, A. Vimont, M. Daturi, P. Horcajada and C. Serre, *Chem. Commun.*, 2013, **49**, 7773–7775.

118 M. Ma, H. Noei, B. Mienert, J. Niesel, E. Bill, M. Muhler, R. A. Fischer, Y. Wang, U. Schatzschneider and N. Metzler-Nolte, *Chem*, 2013, **19**, 6785–6790.

119 M. J. Ingleson, R. Heck, J. A. Gould and M. J. Rosseinsky, *Inorg. Chem.*, 2009, **48**, 9986–9988.

120 S. A. Baudron, *CrystEngComm*, 2010, **12**, 2288–2295.

121 C. Kim, S. Diring, S. Furukawa and S. Kitagawa, *Dalton Trans.*, 2015, **44**, 15324–15333.

122 S. Diring, A. Carne-Sanchez, J. Zhang, S. Ikemura, C. Kim, H. Inaba, S. Kitagawa and S. Furukawa, *Chem. Sci.*, 2017, **8**, 2381–2386.

123 Z. Jin, P. Zhao, J. Zhang, T. Yang, G. Zhou, D. Zhang, T. Wang and Q. He, *Chem. – Eur. J.*, 2018, **24**, 11667–11674.

124 Q. Guan, L. L. Zhou, Y. A. Li and Y. B. Dong, *Chem. Commun.*, 2019, **55**, 14898–14901.

125 S. Diring, D. O. Wang, C. Kim, M. Kondo, Y. Chen, S. Kitagawa, K.-I. Kamei and S. Furukawa, *Nat. Commun.*, 2013, **4**, 917–935.

126 V. V. Vinogradov, A. S. Drozdov, L. R. Mingabudinova, E. M. Shabanova, N. O. Kolchina, E. I. Anastasova, A. A. Markova, A. A. Shtil, V. A. Milichko, G. L. Starova, R. L. M. Precker, A. V. Vinogradov, E. Hey-Hawkins and E. A. Pidko, *J. Mater. Chem. B*, 2018, **6**, 2450–2459.

127 L.-C. Yu, Z.-F. Chen, C.-S. Zhou, H. Liang and Y. Li, *J. Coord. Chem.*, 2005, **58**, 1681–1687.

128 K. M. P. William, J. Rieter, K. M. L. Taylor and W. Lin, *J. Am. Chem. Soc.*, 2008, **130**, 11584–11585.

129 R. C. Huxford, W. S. Boyle, D. Liu and W. Lin, *Chem. Sci.*, 2012, **3**, 198–204.

130 D. Liu, S. A. Kramer, R. C. Huxford-Phillips, S. Wang, J. Della Rocca and W. Lin, *Chem. Commun.*, 2012, **48**, 2668–2670.

131 R. C. Huxford-Phillips, S. R. Russell, D. Liu and W. Lin, *RSC Adv.*, 2013, **3**, 14438–14443.

132 D. Liu, C. Poon, K. Lu, C. He and W. Lin, *Nat. Commun.*, 2014, **5**, 4182–4192.

133 C. He, D. Liu and W. Lin, *Biomaterials*, 2015, **36**, 124–133.

134 C. He, D. Liu and W. Lin, *ACS Nano*, 2015, **9**, 991–1003.

135 C. Poon, C. He, D. Liu, K. Lu and W. Lin, *J. Controlled Release*, 2015, **201**, 90–99.

136 C. He, C. Poon, C. Chan, S. D. Yamada and W. Lin, *J. Am. Chem. Soc.*, 2016, **138**, 6010–6019.

137 Y. Yang, Y. Chao, J. Liu, Z. Dong, W. He, R. Zhang, K. Yang, M. Chen and Z. Liu, *NPG Asia Mater.*, 2017, **9**, e344.

138 K. Ni, G. Lan, S. S. Veroneau, X. Duan, Y. Song and W. Lin, *Nat. Commun.*, 2018, **9**, 4321–4333.

139 C. Chan, N. Guo, X. Duan, W. Han, L. Xue, D. Bryan, S. C. Wightman, N. N. Khodarev, R. R. Weichselbaum and W. Lin, *Biomaterials*, 2019, **210**, 94–104.

140 X. Duan, C. Chan, W. Han, N. Guo, R. R. Weichselbaum and W. Lin, *Nat. Commun.*, 2019, **10**, 1899–1913.

141 Y. Yang, J. Liu, C. Liang, L. Feng, T. Fu, Z. Dong, Y. Chao, Y. Li, G. Lu and M. Chen, *ACS Nano*, 2016, **10**, 2774–2781.

142 J. Wu, Y. Hu, H. Ye, S. Zhang, J. Zhu, D. Ji, Y. Zhang, Y. Ding and Z. Huang, *JACS Au*, 2022, **2**, 2339–2351.

143 K. Lu, C. He and W. Lin, *J. Am. Chem. Soc.*, 2014, **136**, 16712–16715.

144 K. Lu, C. He and W. Lin, *J. Am. Chem. Soc.*, 2015, **137**, 7600–7603.

145 K. Lu, C. He, N. Guo, C. Chan, K. Ni, R. R. Weichselbaum and W. Lin, *J. Am. Chem. Soc.*, 2016, **138**, 12502–12510.

146 G. Lan, K. Ni, Z. Xu, S. S. Veroneau, Y. Song and W. Lin, *J. Am. Chem. Soc.*, 2018, **140**, 5670–5673.

147 J. Park, D. Feng, S. Yuan and H.-C. Zhou, *Angew. Chem., Int. Ed.*, 2015, **54**, 430–445.

148 J. Park, Q. Jiang, D. Feng, L. Mao and H.-C. Zhou, *J. Am. Chem. Soc.*, 2016, **138**, 3518–3525.

149 S.-Y. Li, H. Cheng, B.-R. Xie, W.-X. Qiu, J.-Y. Zeng, C.-X. Li, S.-S. Wan, L. Zhang, W.-L. Liu and X.-Z. Zhang, *ACS Nano*, 2017, **11**, 7006–7018.

150 W. Liu, Y.-M. Wang, Y.-H. Li, S.-J. Cai, X.-B. Yin, X.-W. He and Y.-K. Zhang, *Small*, 2017, **13**, 1603459–1603466.

151 Y. Ma, X. Li, A. Li, P. Yang, C. Zhang and B. Tang, *Angew. Chem., Int. Ed.*, 2017, **56**, 13752–13756.

152 B. Li, X. Wang, L. Chen, Y. Zhou, W. Dang, J. Chang and C. Wu, *Theranostics*, 2018, **8**, 4086–4096.

153 J. Wang, Y. Fan, Y. Tan, X. Zhao, Y. Zhang, C. Cheng and M. Yang, *ACS Appl. Mater. Interfaces*, 2018, **10**, 36615–36621.

154 J.-Y. Zeng, M.-Z. Zou, M. Zhang, X.-S. Wang, X. Zeng, H. Cong and X.-Z. Zhang, *ACS Nano*, 2018, **12**, 4630–4640.

155 K. Zhang, X. Meng, Y. Cao, Z. Yang, H. Dong, Y. Zhang, H. Lu, Z. Shi and X. Zhang, *Adv. Funct. Mater.*, 2018, **28**, 1804634–1804643.

156 W. Zhang, J. Lu, X. Gao, P. Li, W. Zhang, Y. Ma, H. Wang and B. Tang, *Angew. Chem., Int. Ed.*, 2018, **57**, 4891–4896.

157 Y. Zhao, Y. Kuang, M. Liu, J. Wang and R. Pei, *Chem. Mater.*, 2018, **30**, 7511–7520.

158 X. Zheng, L. Wang, M. Liu, P. Lei, F. Liu and Z. Xie, *Chem. Mater.*, 2018, **30**, 6867–6876.

159 S.-S. Wan, Q. Cheng, X. Zeng and X.-Z. Zhang, *ACS Nano*, 2019, **13**, 6561–6571.

160 C. Wang, F. Cao, Y. Ruan, X. Jia, W. Zhen and X. Jiang, *Angew. Chem., Int. Ed.*, 2019, **58**, 9846–9850.

161 X. Zhao, Z. Zhang, X. Cai, B. Ding, C. Sun, G. Liu, C. Hu, S. Shao and M. Pang, *ACS Appl. Mater. Interfaces*, 2019, **11**, 7884–7892.

162 L. Zhang, J. Lei, F. Ma, P. Ling, J. Liu and H. Ju, *Chem. Commun.*, 2015, **51**, 10831–10834.

163 T. V. Slenters, I. Hauser-Gerspach, A. U. Daniels and K. M. Fromm, *J. Mater. Chem.*, 2008, **18**, 5359–5362.

164 O. Gordon, T. Vig Slenters, P. S. Brunetto, A. E. Villaruz, D. E. Sturdevant, M. Otto, R. Landmann and K. M. Fromm, *Antimicrob. Agents Chemother.*, 2010, **54**, 4208–4218.

165 M. Berchel, T. L. Gall, C. Denis, S. L. Hir, F. Quentel, C. Elléouet, T. Montier, J.-M. Rueff, J.-Y. Salaün, J.-P. Haelters, G. B. Hix, P. Lehn and P.-A. Jaffrès, *New J. Chem.*, 2011, **35**, 1000–1003.

This journal is © The Royal Society of Chemistry 2023

J. Mater. Chem. B, 2023, **11**, 3273–3294 | **3293**

166 R. E. F. de Paiva, C. Abbehausen, A. F. Gomes, F. C. Gozzo, W. R. Lustri, A. L. B. Formiga and P. P. Corbi, *Polyhedron*, 2012, **36**, 112–119.

167 S. W. Jaros, P. Smoleński, M. F. C. Guedes da Silva, M. Florek, J. Król, Z. Staroniewicz, A. J. L. Pombeiro and A. M. Kirillov, *CrystEngComm*, 2013, **15**, 8060–8064.

168 K. Wang, X. Ma, D. Shao, Z. Geng, Z. Zhang and Z. Wang, *Cryst. Growth Des.*, 2012, **12**, 3786–3791.

169 C. Chiericatti, J. C. Basilico, M. L. Zapata Basilico and J. M. Zamaro, *Microporous Mesoporous Mater.*, 2012, **162**, 60–63.

170 W. Zhuang, D. Yuan, J.-R. Li, Z. Luo, H.-C. Zhou, S. Bashir and J. Liu, *Adv. Healthcare Mater.*, 2012, **1**, 225–238.

171 S. Aguado, J. Quiros, J. Canivet, D. Farrusseng, K. Boltes and R. Rosal, *Chemosphere*, 2014, **113**, 188–192.

172 S. A. Ahmed, D. Bagchi, H. A. Katouah, M. N. Hasan, H. M. Altass and S. K. Pal, *Sci. Rep.*, 2019, **9**, 19372–19382.

173 K. Ni, G. Lan, C. Chan, B. Quigley, K. Lu, T. Aung, N. Guo, P. La Riviere, R. R. Weichselbaum and W. Lin, *Nat. Commun.*, 2018, **9**, 1–12.

174 A. D. Burrows, M. Jurcic, M. F. Mahon, S. Pierrat, G. W. Roffe, H. J. Windle and J. Spencer, *Dalton Trans.*, 2015, **44**, 13814–13817.

175 C. Tamames-Tabar, E. Imbuluzqueta, N. Guillou, C. Serre, S. R. Miller, E. Elkaïm, P. Horcajada and M. J. Blanco-Prieto, *CrystEngComm*, 2015, **17**, 456–462.

176 Y. Hu, T. Lv, Y. Ma, J. Xu, Y. Zhang, Y. Hou, Z. Huang and Y. Ding, *Nano Lett.*, 2019, **19**, 2731–2738.

177 J. Liu, Y. Yang, W. Zhu, X. Yi, Z. Dong, X. Xu, M. Chen, K. Yang, G. Lu, L. Jiang and Z. Liu, *Biomaterials*, 2016, **97**, 1–9.

178 K. Ni, T. Aung, S. Li, N. Fatuzzo, X. Liang and W. Lin, *Chem*, 2019, **5**, 1892–1913.

3294 | *J. Mater. Chem. B*, 2023, **11**, 3273–3294

This journal is © The Royal Society of Chemistry 2023